NBER WORKING PAPER SERIES

UNCERTAINTY AND GROWTH DISASTERS

Boyan Jovanovic
Sai Ma

Working Paper 28024
http://www.nber.org/papers/w28024

NATIONAL BUREAU OF ECONOMIC RESEARCH
1050 Massachusetts Avenue
Cambridge, MA 02138
October 2020

We thank Henry Hyatt, Georgui Kambourov, and Iourii Manovskii for data, and Ian Dew-Becker, Martina Hengge, Seung Lee, Milan Nedeljkovic, Sergio Rebelo, and John Rogers for comments and suggestions. All errors are ours. The views expressed are those of the authors and not necessarily those of the Federal Reserve Board, the Federal Reserve System, or the National Bureau of Economic Research.

Uncertainty and Growth Disasters
Boyan Jovanovic and Sai Ma
NBER Working Paper No. 28024
October 2020
JEL No. E3

ABSTRACT

This paper documents several facts on the real effects of economic uncertainty. First, higher uncertainty is associated with a more dispersed distribution of output growth. Second, the relation is highly asymmetric: A rise in uncertainty is associated with a sharp decline in the lower tail of the growth distribution whereas it has a much smaller and insignificant impact on its upper tail. Third, the negative response of growth to uncertainty shocks is larger when the equity market is more volatile. We build a model in which growth and uncertainty are both endogenous: rapid adoption of new technology raises economic uncertainty and may cause measured productivity to decline. The equilibrium growth distribution is negatively skewed and higher uncertainty leads to a thicker left tail and to more labor reallocation among jobs and among

Boyan Jovanovic
New York University
Department of Economics
19 W. 4th Street, 6th Floor
New York, NY 10012
and NBER
Boyan.Jovanovic@nyu.edu

Sai Ma
Federal Reserve Board,
C Ave & 20th Street NW
Washington, DC 20551
sai.ma@frb.gov

1 Introduction

Contemporary macro literature often finds uncertainty about the future to be an important driver of economic fluctuations. A growing body of work proposes uncertainty as a cause of economic slowdowns and sluggish recoveries. For example, Bloom (2009a) and Bloom, Floetotto, Jaimovich, Saporta-Eksten and Terry (2018) argue that higher uncertainty stems from the process governing technological innovation, which subsequently causes a decline in real activity.

Empirically, this evidence has been found to be robust to the use of various proxy variables such as implied stock volatility (VIX), economic policy uncertainty (EPU) from Baker, Bloom and Davis (2016), or a broad-based measure of macroeconomic and financial uncertainty, as in Jurado, Ludvigson and Ng (2015) (JLN) and Ludvigson, Ma and Ng (2019) (LMN). However, these papers usually investigate the impact of higher uncertainty on mean growth either via a linear forecasting regression or a structural vector autoregression (SVAR). Consequently, they are silent about the effect of uncertainty on the volatility or other *higher* moments of the growth distribution, and this may underestimate the impact of economic uncertainty on growth downside risk.

In this paper, we provide evidence that uncertainty is highly correlated with the higher moments of the growth distribution. Figure 1 depicts the contemporaneous relationship between JLN macro uncertainty and 36-month rolling window average growth of industrial production (hereafter "IP") in the left panel, IP growth *volatility* in the middle panel, and IP growth *skewness* in the right panel. While uncertainty is highly negatively correlated (-36%) with mean growth as the literature has shown, we find that uncertainty is also highly correlated with growth volatility (44%) and growth skewness (-22%). Therefore, higher uncertainty is not only associated with lower mean growth but also contributes to a more dispersed and negatively skewed growth distribution.

We estimate the distribution of future real growth of IP as a function of uncertainty measures using quantile regression methods.[1] We document three stylized facts. First, higher economic uncertainty is associated with a more dispersed and left-skewed future growth distribution. A one-standard-deviation increase in uncertainty statistically significantly increases the interquartile range of the one-month ahead annualized growth distribution by 2%, and decreases the lower 5th percentile by 5%. This indicates that the marginal effects of higher uncertainty are to significantly increase growth downside risk.

[1] This empirical model is based on Adrian, Boyarchenko and Giannone (2019) (ABG). Instead of using an uncertainty measure, ABG uses the national financial condition index (NFCI) as the conditioning variable to estimate the growth distribution.

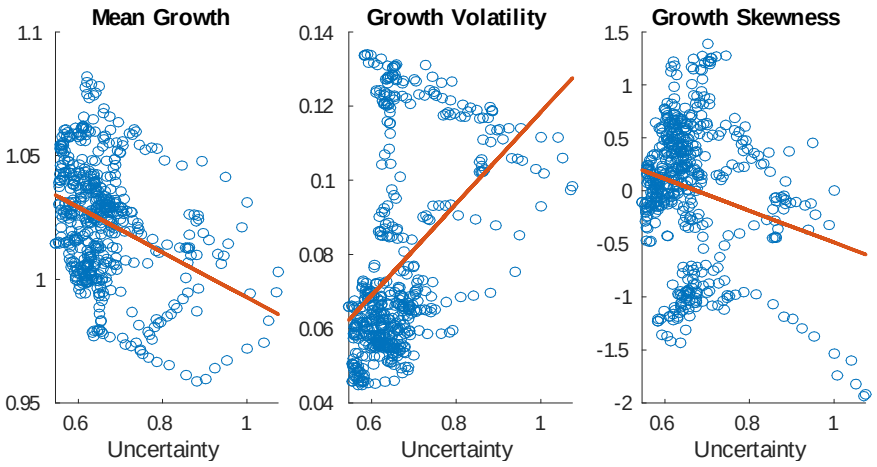

Figure 1: Uncertainty and Higher Moments of Growth. Note: this figure depicts the contemporaneous relationship between JLN macro uncertainty and 36-month rolling window average industrial production (IP) growth (left panel), growth volatility (middle panel), and growth skewness (right panel). The sample spans the period 1973:01 to 2018:12.

Second, the response of IP growth to changes in uncertainty is highly asymmetric, the response being much higher when uncertainty rises than when it falls. An increase in uncertainty is associated with a larger decrease in the lower tail of the growth distribution while it has a much smaller impact on its upper tail. These results suggest that higher uncertainty could lead to an abrupt economic decline whereas lower uncertainty does not necessarily rebound the economy from the recession. Third, higher asset volatility magnifies the negative impact of uncertainty on growth. We find that when the equity market is more volatile as measured by a higher VIX, an increase in macro uncertainty has a larger negative impact on the lower tail of the expected growth distribution. A one-standard deviation increase in VIX increases in the marginal effect of uncertainty on the lower 5th percentile by 10%.

Motivated by this evidence, we present and estimate an endogenous growth model that generates uncertainty. Equilibrium growth results from the adoption of technologies of uncertain quality. A technology's "quality" refers to how closely the technology's needs match the economy's input endowments. Since technology needs are unpredictable, its rapid irreversible adoption raises uncertainty and can even lead to a decline in output and, hence, to negative growth.

Uncertainty thus affects growth because of technological commitment and the *ex-post* mismatch between the technology and the firm's inputs. Firms adopt technologies the exact character of which they do not know; a firm may have to commit to the scale of its factory and to the size of its labor force, as argued by Ramey and Ramey (1991), or it

may be have to commit to the skill and occupational composition of the labor force. The mismatch is distributed symmetrically but the *cost* of that mismatch is quadratic so that maximal losses from technology adoption exceed the maximal gains. The firm's growth rate is therefore negatively skewed as observed in the data.

How well a technology fits a firm's asset endowments is revealed only after the fact. An ex-post mismatch causes a resulting adjustment which we hypothesize will show up in job-to-job mobility whereby workers move from one firm to another, and in occupational mobility which may also be internal to the firm when it reallocates workers among tasks that differ in their occupational label.

The model provides an analytic characterization of the equilibrium growth distribution. Consistent with our empirical evidence, higher uncertainty about the newly adopted technologies leads to a lower average growth as well as a more dispersed and negatively skewed growth distribution. By assuming that the uncertainty has no *long-run* impacts on growth, the calibrated model is able to quantitatively match the marginal effect of uncertainty on several key moments of the growth distribution. As in the data, the model suggests that higher asset price volatility, measured from the estimated option prices of a Lucas (1978) representative security, leads to a higher marginal effect of uncertainty on the lower tail of the growth distribution.

Related Literature

Our paper relates closely to two major strands of literature. First, a growing body of *empirical* studies the real effect of uncertainty. Carriero, Clark and Marcellino (2018) finds that economic uncertainty has a strong negative effect on economic outcomes. Similarly, based on breaks in the volatility of macroeconomic variables, Angelini, Bacchiocchi, Caggiano and Fanelli (2019) shows that macro uncertainty has a contractionary effect on output. Using a shock-restricted SVAR approach, Ludvigson et al. (2019) finds that financial uncertainty is a possible source of business cycle fluctuations. In spite of the mixed evidence on which type of uncertainty has a contractionary effect on economic growth, it's evident that the higher uncertainty about future economic conditions exhibits a large impact on mean growth. However, all these papers investigate uncertainty and real variables using a structural vector autoregression (SVAR) framework and thus cannot establish a relationship between uncertainty and higher moments of the growth distribution.[2]

One exception is Hengge (2019). As we do in our paper, she also uses quantile re-

[2]Other examples include Baker and Bloom (2013), Caldara, Fuentes-Albero, Gilchrist and Zakrajšek (2016), Alfaro, Bloom and Lin (2016), and Shin and Zhong (2018).

gression analysis and shows that the relationship between macroeconomic uncertainty and future quarterly GDP growth is highly nonlinear and asymmetric. Our empirical evidence on the asymmetric response of expected IP growth to higher uncertainty is consistent with hers despite our use of monthly IP as the measure of economic growth. Using quantile regression estimates, we further construct the Growth-at-Risk measure and study its interaction with asset pricing volatility and capacity utilization both empirically and theoretically. To the best of our knowledge, we are the first to provide a theoretical framework to study the impact of uncertainty on higher moments of the growth distribution.

Second, a large body of *theoretical* literature proposes that higher economic uncertainty causes lower output growth. Prescott and Visscher (1980) argue that workers' comparative advantages for performing various tasks differ and firms need to learn them at a cost. If a new technology garbles their aptitudes for some of the workers, this gives rise to a reallocation cost that lowers output. More generally, there are models of the real options effects of uncertainty (Bernanke (1983), McDonald and Siegel (1986)), models in which uncertainty influences financing constraints (Gilchrist, Sim and Zakrajsek (2010), Arellano, Bai and Kehoe (2011)), investment (Fajgelbaum, Schaal and Taschereau-Dumouchel (2017)), or precautionary saving (Basu and Bundick (2017), Leduc and Liu (2016), Fernández-Villaverde, Pablo Guerrón-Quintana and Uribe (2011), Bianchi, Kung and Tirskikh (2018)). Our notion of uncertainty in the model is similar to Bloom (2009a) and Bloom et al. (2018) that assume that higher uncertainty originates directly in the process governing technological innovation and adoption.

Our paper is also related to papers on disaster risk and business cycles. Gourio (2012) studies the impact of disastrous shocks on the first moments of real variables whereas our paper focuses on the second and third moments. Related to our findings, Berger, Dew-Becker and Giglio (2020) and Dew-Becker, Tahbaz-Salehi and Vedolin (2020) theoretically and empirically emphasize the importance of time-varying second moment and skewness in thinking about uncertainty shocks.

Our model follows the putty-clay tradition of Johansen (1959), and assumes irreversible technological commitment, building on Ramey and Ramey (1991) and Jovanovic (2006). It derives closed-form expressions for equilibrium growth and its distribution, and studies the relationship between uncertainty and higher moments of the growth distribution. Central to the model is investment in intangible capital which McGrattan and Prescott (2014) and Bhandari and McGrattan (2018) estimate to be sixty percent of firms' total assets. Parente (1994) and Klenow (1998) explain asymmetry at the level of the firm by assuming that a technology improves with use through learning by doing. Upon an

update, productivity drops sharply and then recovers gradually.

Closely related is Ramey and Ramey (1991) which, in a one-period model also assumes technological commitment so that output may decline when new technology is adopted, and where greater variability of shocks reduces expected output. In Chalkley and Lee (1998), Veldkamp (2005), and Fajgelbaum et al. (2017) agents observe shocks more accurately when investment is high and therefore in a boom a negative shock to the efficiency of investment is quickly detected and so, when a bad shock hits, investment suddenly drops. Thus, a negative TFP shock in a boom has a quicker impact than a positive shock does in a slump – investment responds asymmetrically to a symmetric exogenous shocks because firms can detect negative shocks more quickly than positive ones. Our paper shares the feature that uncertainty is endogenous – agents' actions affect how uncertain they feel about future macroeconomic variables.

The rest of this paper is organized as follows. Section 2 provides evidence on the asymmetric real effects of uncertainty. Section 3 presents the model, and analyzes its empirical implications. Section 4 adds three extensions: A Markov-switching process for a parameter that influences the level of uncertainty induced by technological upgrading , an alternative measure for aggregate output, and recursive preferences. Section 5 concludes the paper.

2 Empirical Evidence

In this section, we describe the data and present the key empirical fact that the relationship between future economic growth and uncertainty is highly nonlinear. To document this feature in the data, we follow Adrian et al. (2019) and investigate the relationship between uncertainty and future growth via forecasting quantile regressions. Compared to the traditional OLS forecasting regressions, quantile regressions describe how the set of conditional variables, including uncertainty measures, affect different quantiles of the future growth. This methodology thus allows the estimated relationship between uncertainty and future growth to differ across quantiles. This extension of a simple linear regression model can capture the potential nonlinear relationship between the shocks in uncertainty and vulnerability of the growth, which is largely neglected in the literature. More formally, we regress the h-month-ahead real IP growth (hereafter "IP growth") on a vector of condition variables $\mathbf{X}_t$,

$$\Delta ip_{t+h,\alpha} = \boldsymbol{\delta}'_{\alpha,h}\mathbf{X}_t + \varepsilon_t, \tag{1}$$

where the conditional variables $\mathbf{X}_t$ include a constant, the lag of the IP growth, and uncertainty U_t.

The regression slope can be obtained by minimizing the quantile-weighted absolute value of errors:

$$\hat{\boldsymbol{\delta}}_{\alpha,h} = \arg\min \sum_t \left\{ \begin{array}{c} \alpha \mathbf{1}_{\Delta ip_{t+h,\alpha} > \boldsymbol{\delta}'_{\alpha,h}\mathbf{x}_t} \left|\Delta ip_{t+h,\alpha} - \boldsymbol{\delta}'_{\alpha}\mathbf{x}_t\right| \\ + (1-\alpha)\, \mathbf{1}_{\Delta ip_{t+h,\alpha} < \boldsymbol{\delta}'_{\alpha,h}\mathbf{x}_t} \left|\Delta ip_{t+h,\alpha} - \boldsymbol{\delta}'_{\alpha}\mathbf{x}_t\right| \end{array} \right\}, \tag{2}$$

where h is the forecasting horizon, α is the quantile and $\mathbf{1}$ is the indicator variable. For inference, standard errors are estimated via the bootstrap procedure described in Adrian et al. (2019).

2.1 Data

The monthly IP data is obtained from FRED Economic database maintained by the Federal Reserve Bank of St. Louis. Our main measure of uncertainty, denoted by U_t^M, is the macroeconomic uncertainty index from Jurado et al. (2015) (hereafter JLN uncertainty), which aggregates over a large number of individual uncertainties constructed from a panel of data. More specifically, let $y_{jt}^M \in Y_t^M = (y_{1t}^M, \ldots, y_{N_C t}^M)'$ be a variable in a set of large macroeconomic series denoted by Y_t^M. For each macro series y_{jt}^M, its h-period ahead uncertainty, denoted by $\mathcal{U}_{jt}^M(h)$, is defined to be the volatility of the purely unforecastable component of the future value of the series, conditional on all information available. Specifically,

$$\mathcal{U}_{jt}^M(h) \equiv \sqrt{\mathbb{E}\Big[(y_{jt+h}^M - \mathbb{E}[y_{jt+h}^M|I_t])^2|I_t\Big]},$$

where I_t denotes the information available up to time t. Then h-period macro uncertainty $\mathcal{U}_{jt}^M(h)$ is an aggregate of individual uncertainty measures across all macro series:

$$U_t^M(h) \equiv \text{plim}_{N_M\to\infty} \sum_{j=1}^{N_M} \frac{1}{N_M} \mathcal{U}_{jt}^M(h) \equiv \mathbb{E}[\mathcal{U}_{jt}^M(h)].$$

For JLN macro uncertainty, they use a monthly macro dataset consisting of $N_M = 134$ mostly macroeconomic time series listed in McCracken and Ng (2016). Intuitively, if the expectation of the squared error in forecasting y_{jt+h} rises, uncertainty in that variable increases. In this paper, we update JLN uncertainty index to 2018:12 and use the one-month ahead ($h = 1$) macro uncertainty as our baseline measure of uncertainty, following Ludvigson et al. (2019). Our sample is monthly and spans the period 1973:01 to 2018:12, unless otherwise noted.

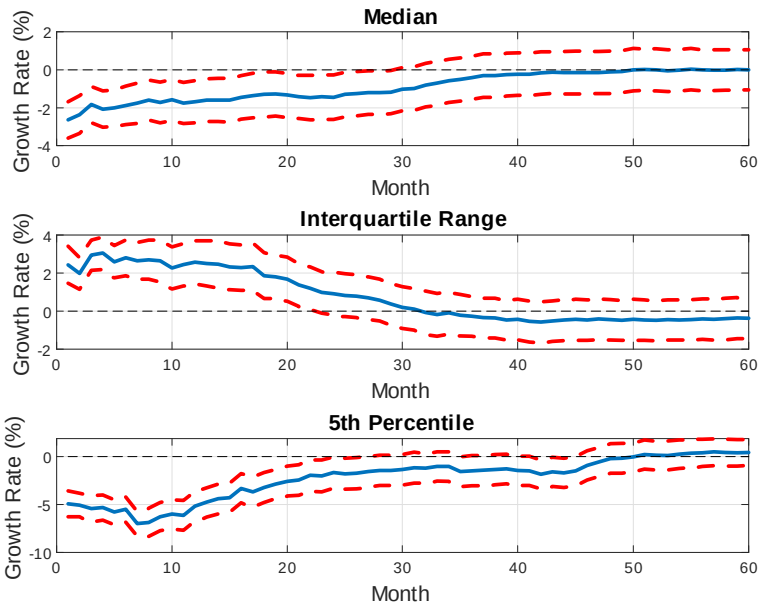

Figure 2: Impact of a one-standard deviation increase in uncertainty measure on the annualized growth rate. Note: this figure report the estimated coefficient of uncertainty over $h = 1, 2..., 60$ months from the baseline quantile regression described in the texts. The bootstrapped 68% confidence intervals are reported in red dashed lines.

2.2 Results

By construction, any effects of changes in $\mathbf{x}_t$ on h-month ahead growth at α percentile is captured by the slope estimate $\hat{\boldsymbol{\delta}}_{\alpha,h}$. Figure 2 reports the estimates of marginal coefficient of uncertainty over $h = 1, 2..., 60$ months.[3] The top panel reports the effect of uncertainty on changes in expected median growth. We find that a one-standard-deviation increase in uncertainty decreases the median of the annualized growth by 3% over the next month. The effect gradually weakens over time with a half-life of 23 months. The middle panel shows that the distribution of the growth becomes more *dispersed* following an increase in uncertainty. The interquartile range (75th minus 25th percentile) rises at short- and medium- terms. Similarly, the bottom panel shows that when uncertainty increases, the distribution of the growth is more negatively skewed. The 5th percentile of the growth falls by 6% at short horizon, and 2% over 2 to 4 years. As a result, the impact of the uncertainty on skewness of the distribution is long-lasting.

In Figure 3, we plot the estimated uncertainty coefficients $\boldsymbol{\delta}_{\alpha,h}$ for different α over

[3] One can interpret the cofficients from equation (1) over h as the impulse responses to uncertainty shock, as in the local projection method from Jordà (2005).

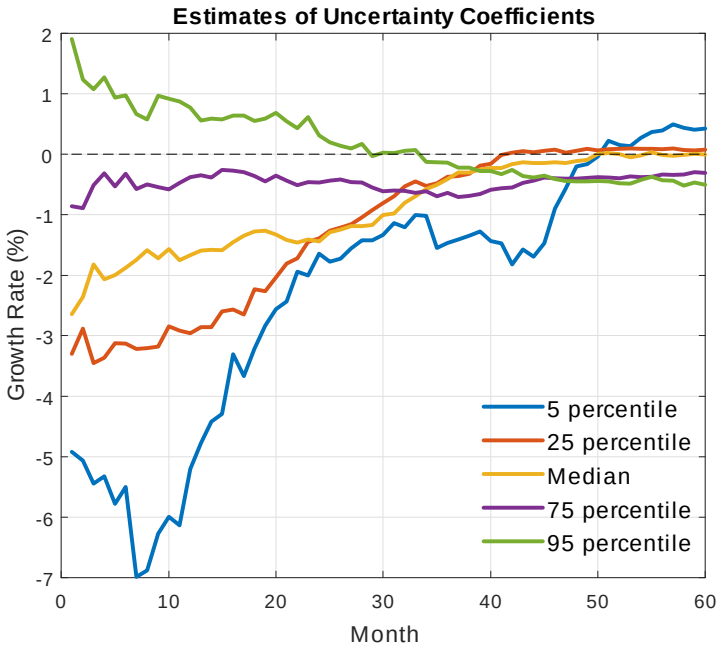

Figure 3: Asymmetric impact of uncertainty on growth. Note: this figure reports the estimated uncertianty coefficients for different quantiles α over horizon h from the baseline quantile regression described in the texts.

horizon h. In most cases, an increase in uncertainty is associated with a larger decrease in the lower tail of the growth distribution while it has much smaller impact on the upper tail. This asymmetric response shows that the impact of uncertainty on growth is highly nonlinear.

2.3 Growth-at-Risk

We define Growth-at-Risk (GaR) as the lower 5th percentile of the estimated conditional distribution of real IP growth. It's worth noting that our measure of GaR differs from the one in Adrian, Grinberg, Liang and Malik (2018) because they use the national financial condition index (NFCI) from the Chicago Fed in conditional variables x_t whereas we use the uncertainty measure.[4] In fact, in Appendix 6, we show that JLN uncertainty has more accurate out-of-sample forecast of IP growth distribution (i.e. higher average predictive scores) than NFCI. Figure 4 shows the time series of one-month ahead GaR estimated using uncertainty measure. The red line in the figure shows the he GaR estimated using NFCI for comparisons. First, it shows that both measures of GaR are counter-cyclical

[4]In addition, Adrian et al. (2018) uses quarterly GDP growth to measure of economic growth whereas we use monthly IP growth.

and with a less than 5% probability, a one-standard deviation increase in uncertainty is associated with as much as a 3% decline in IP Growth within a month during recessions. Second, GaR estimated with uncertainty is more volatile and exhibit larger spikes during recessions. For the rest of the paper, we refer to GaR as the one that is estimated using uncertainty.

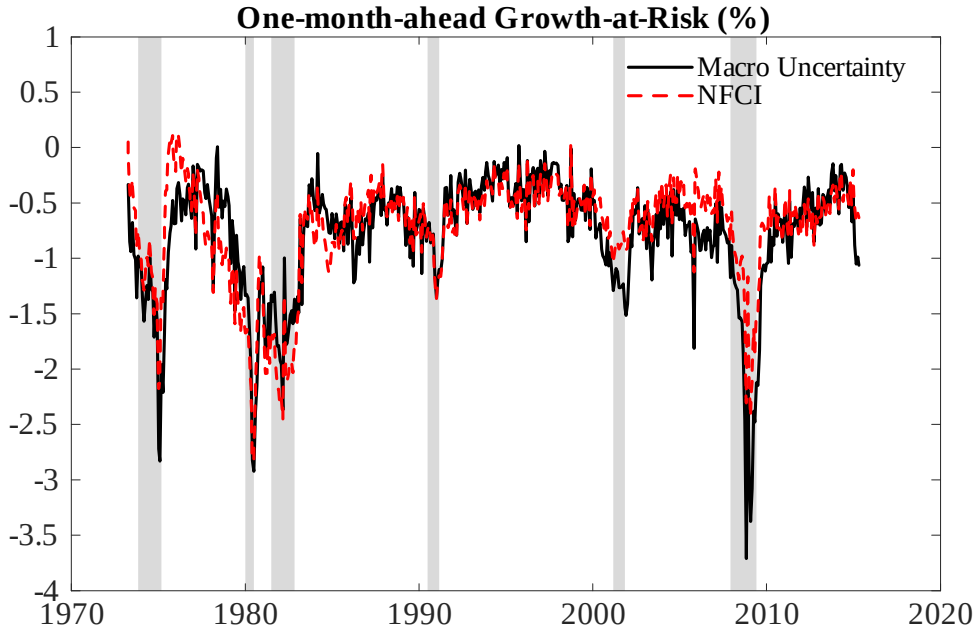

Figure 4: Growth-at-Risk. Note: this figure reports the estimated Growth-at-Risk using NFCI (red line) and JLN Macro uncertainty (black line). The baseline quantile regression is described in the texts. The sample spans the period 1973:01 to 2018:12.

Our baseline measure of uncertainty is based on macro variables but some papers in the literature, such as Ludvigson et al. (2019), found evidence that volatility related to the asset returns also lead to persistent decline IP growth. This evidence suggests that the uncertainty should be associated with a larger decline in growth when asset prices are more volatile. To directly test this argument, Figure 4 plots the estimated GaR against the standardized implied volatility indices (VIX), which is a popular measure of the stock market's expectation of volatility implied by S&P 500 index options.[5] It shows that when the US equity market is more volatile, an increase in macro uncertainty has a larger negative impact on IP growth and thus leads to a lower GaR. On average, a two-standard-deviation increase in VIX is associated with a 0.5% decline in GaR.

[5]In the paper, we chose to use the VXO implied volatility index that is available since 1962 instead of VIX because the latter is only available after 1990 and the two measures are 99% correlated.

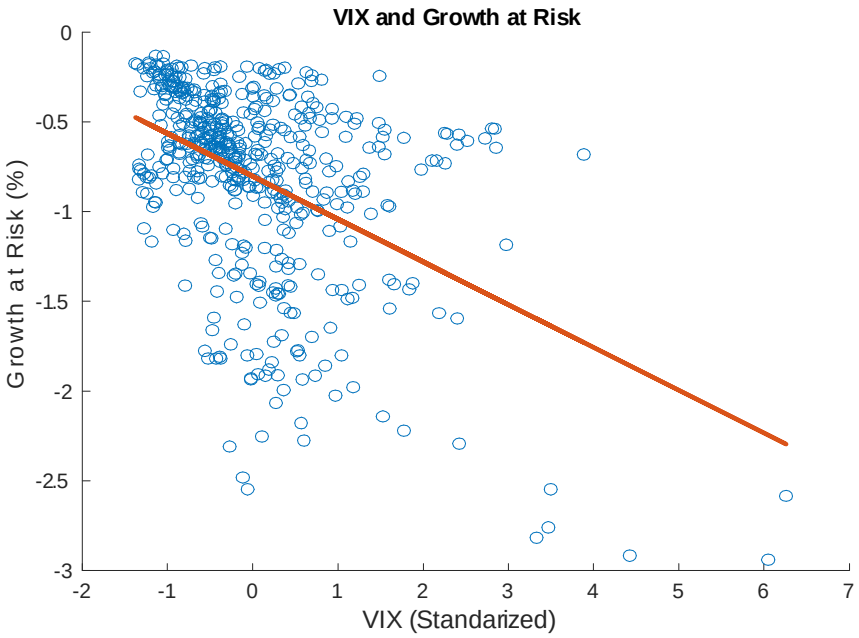

Figure 5: Growth-at-Risk and VIX. Note: this figure shows the contempraneous relationship between standardized VIX and estimated Growth-at-Risk. The Growth-at-Risk is estimated conditional on JLN macro uncertainty. The red line reports the OLS Estimate. The sample spans the period 1973:01 to 2018:12.

To sum up, we document some empirical evidence on the real effect of uncertainty. First, we find that an increase in uncertainty leads to lower median and yet more volatile IP growth, and a more negative GaR. Second, the response of IP growth to an increase in uncertainty is highly nonlinear, especially at the short term. Third, higher asset volatility magnifies a negative effect of uncertainty on growth. The next section presents an endogenous growth model that captures these facts.

3 Model

The following model endogenizes growth and uncertainty. It features a collection of agents that can raise their productivities by adopting new technologies. We first focus on a single agent and then in Sec. 3.1 discuss why the representative agent assumption holds up in a group of agents in spite of the informational spillovers involved. Consider an agent "Crusoe," with preferences over consumption sequences (c_t)

$$E_0 \left\{ \sum_0^\infty \beta^t \ln c_t \right\}.$$

We use log utility here for analytical tractability. In Section 4.3, we extend the model using Epstein and Zin (2013) recursive preferences and show that it delivers the same economic insights.

Production.— For simplicity of the exposition, we assume there is a single production good y and there is no physical capital. The output depends on the level of technology A as well as Crusoe's skill mix h. The potential output, y^p, is defined as

$$y^p = \exp\left\{A - \frac{\lambda}{2}\left(s_A - h'\right)^2\right\}. \tag{3}$$

where s_A is the skill-mix ideal for technology A. By construction, $\frac{\lambda}{2}\left(s_A - h'\right)^2$ captures the foregone output due to the "skill gap" between Crusoe's current skill and the ideal skill for technology A.

Adoption of Technology.— Crusoe can raise his technology by any amount, $x \geq 0$, so that starting today at A, tomorrow's technology is

$$A' = A + x.$$

Crusoe must use technology A' for at least one period. We assume that adopting a new technology is free but adoption of the new technology A' makes unpredictable demands on the skill mix,

$$s_{A'} = s_A + x\varepsilon, \tag{4}$$

where $\varepsilon \sim F(\varepsilon)$ is *time* specific and i.i.d., having mean zero and variance σ^2. Once ε is drawn, $s_{A'}$ becomes an invariant skill requirement for technology A'. Crusoe chooses A' before seeing ε, and he can*not* return to technologies that he used in the past.

Adjustment of h.—Crusoe starts the period with h. Before producing, he can change it to $h' \equiv h + \Delta$ at an adjustment cost of

$$C\left(y^p, \Delta\right) \equiv \left[1 - \exp\left\{-\frac{\theta}{2}\Delta^2\right\}\right] y^p.$$

Finally, Crusoe's net output is

$$y^p - C\left(y^p, \Delta\right) \equiv y\left(u, \Delta, A\right) = \exp\left\{A - \frac{\lambda}{2}\left(u - \Delta\right)^2 - \frac{\theta}{2}\Delta^2\right\}, \tag{5}$$

where

$$u = s_A - h, \tag{6}$$

is the gap between ideal and actual skill (hereafter the "skill gap").

3.1 Optimal Investment in skill and in technological upgrading

Crusoe's state is his skill gap u and technology level A. His decisions are (x, Δ). He has no assets other than h and A, and he simply consumes his output. His Bellman equation is

$$V(u, A) = \max_{x,\Delta} \left\{ \ln y(u, \Delta, A) + \beta \int V(u + x\varepsilon - \Delta, A + x)\, dF(\varepsilon) \right\}. \tag{7}$$

The following result is proved in Jovanovic (2006, Proposition 1), but in Proposition 3 we shall generalize it to the case in which the parameter σ follows a two-state Markov process, and in Proposition 5 we shall partially generalize it to cover recursive preferences with an intertemporal elasticity of substitution different from unity. The solution to (7), derived in Appendix 1, can be summarized as follows:

Proposition 1 *The policy functions are*

$$x = \frac{1}{\theta\sigma^2 (1-\beta)(1-\alpha)}, \tag{8}$$

and

$$\Delta = (1-\alpha)\, u, \tag{9}$$

where

$$\alpha = \frac{1}{2\beta} \left\{ 1 + \beta + \frac{\lambda}{\theta} - \sqrt{\left(1 + \beta + \frac{\lambda}{\theta}\right)^2 - 4\beta} \right\}, \tag{10}$$

is the fraction of the gap that Crusoe leaves open. The solution for V is

$$V(u, A) = \frac{A}{1-\beta} - \frac{1}{2}\theta(1-\alpha)\, u^2 + J, \tag{11}$$

where

$$J = \frac{\beta}{1-\beta} \left(\frac{x}{1-\beta} - \left[\frac{\psi}{1-\beta\alpha^2} \right] x^2\sigma^2 \right), \quad \textit{and} \quad \psi = \frac{1}{2} \left(\lambda\alpha^2 + \theta(1-\alpha)^2 \right). \tag{12}$$

Thus Crusoe upgrades technology at a constant rate x, and his adjustment of skills Δ is proportional to his current skill gap u. As a result, using equation (4) and (6), the skill gap u follows a AR(1) process as follows,

$$u_{t+1} = \alpha u_t + x\varepsilon_{t+1}. \tag{13}$$

Reductions in σ are expansionary.—Eq. (8) states that if σ falls, x rises. If a more predictable policy lowers σ that would have an expansionary effect. In line with this prediction, Gulen and Ion (2016) use a news-based index of policy uncertainty and show

that higher uncertainty reduces investment, especially in industries where investment is irreversible – as investment in A is in our model. Similarly, Mody and Nedeljkovic (2018) stress the expansionary effect of unambiguous ECB monetary policy during the Euro Crisis. In Sec. 4.1 we shall extend the model and assume a Markov switching process for σ^2 and study the effect of periodic switches in σ^2 that are not expected to remain fixed forever and there, too, periodic reductions in σ are expansionary.[6]

Uncertainty.—Our notion of uncertainty is captured by the volatility of the skill gap u. Because α is between zero and one, u_t is stationary and its variance is

$$\tau \equiv Var\left(u\right) = \frac{x^2\sigma^2}{1-\alpha^2} = \left(\left(1-\beta\right)^2\left(1-\alpha^2\right)\theta^2\left(1-\alpha\right)^2\right)^{-1}\sigma^{-2}, \tag{14}$$

where the second equality derives from equation (8). Conditional on the current skill gap u, the rise in x prompted by a lower σ, leads to higher uncertainty. On the other hand, an increase in λ, or penalty for skill mismatch, lowers investment x and lowers uncertainty. From equation (14), it's noteworthy that uncertainty τ is a linear function of the parameter σ^{-2}, we therefore consider changes in parameter σ^{-2} as a shock to uncertainty in the rest of this section. Intuitively, a lower σ increases new technology adoption through a higher x; consequently, it becomes harder for Crusoe to predict next-period skill mix $s_{A'}$, and uncertainty hence rises.

Decentralization of the optimum.—All agents start in the same state (u, A) and if they all then take the same actions, the equilibrium is symmetric and it has only aggregate risk. At each date the choice of x and the realization of ε on the RHS of Eq. (13) would then be the same for all agents and there would be no benefit to ex-post reallocation of h. Section 4 of Jovanovic (2006) analyzes the incentives of agents to deviate from this situation by considering the option to "wait and see" how other firms fare with the newly adopted technology. The decentralized version assumes that there are two markets: A market for output, and a market for firm's shares – the only assets available to households. Firms maximize shareholder utility and still reject the option to wait and see the realization of u' before committing to A'. It also assumes that agents are measure zero, and that a deviation from equilibrium actions not change the aggregate state and, particularly, the beliefs of the representative agent.[7]

[6] This in contrast to the effects of a mean-preserving spread in TFP shocks in Jones, Manuelli, Siu, and Stacchetti (2005), who find that through the orecautionary savings channel (which is absent here) this can raise average growth under some conditions.

[7] By contrast, in finite-player one-arm bandit models such as Bolton and Harris (1999) and Keller, Rady and Cripps (2005), a player's actions do affect the beliefs of others, and a player takes the reactions of others into account. In both these models the unknown state is binary and player types remain the

3.2 Growth Distribution

Suppose that $C(y^p, \Delta)$ consists entirely of foregone output. As Appendix 1 also shows, the log of measured output then is,

$$\begin{aligned} \ln y_t &= A - \frac{\lambda}{2}\alpha^2 u_t^2 - \frac{\theta}{2}(1-\alpha)^2 u_t^2 \\ &= A_0 + xt - \psi u_t^2, \end{aligned} \tag{15}$$

where ψ is given in Eq. (12).[8] Because u_t is stationary, $\ln y$ is trend-stationary; the trend and the long-run rate of output growth is x. Growth can be expressed as,

$$g_{t+1} \equiv \ln y_{t+1} - \ln y_t = x - \psi\left(u_{t+1}^2 - u_t^2\right). \tag{16}$$

Eq. (16) shows that growth is driven not just by the adoption of new technology, x, but also by the changes in Crusoe's skill gap $u_{t+1}^2 - u_t^2$. On the one hand, a decrease in the skill gap stimulates growth. On the other hand, adjusting h towards its technologically ideal value is costly and will therefore take time, and output will fall sharply whenever an unlucky draw of s_A occurs. So we should expect the growth distribution to be negatively skewed especially when θ is large. This leads to the following proposition, proved in Appendix 2.

Proposition 2 *Conditional on initial output and technology level y_0 and A_0, if ε_t follows a normal distribution $N(0, \sigma^2)$, the distribution of growth g_t is left skewed and is expressed as*

$$g_t = x - \psi\left[C_t + \left(1-\alpha^2\right)\tau\xi_t^2 + \left(\alpha A_t - B_t\right)\alpha^t u_0 \xi_t\right],$$

where $\xi_t \sim N(0,1)$ follows standard normal distribution and

$$\begin{aligned} A_t &= \sqrt{4(1-\alpha^2)\tau\left(\frac{1-\alpha^{2t}}{1-\alpha^2}+1\right)} \\ B_t &= \sqrt{4(1-\alpha^2)\tau\left(\frac{1-\alpha^{2t}}{1-\alpha^2}\right)} \\ C_t &= \left(\alpha^t u_0\right)^2 - \left(\alpha^{t-1}u_0\right)^2 \\ u_0 &= \sqrt{\frac{1}{\psi}\left(lny_0 - A_0\right)^2}. \end{aligned}$$

same, both in the symmetric equilibria (which sometimes do exist) and asymmetric equilibria that can Pareto dominate the symmetric outcome. In those models, however, there is no counterpart to our variable u; indeed, u would become different for players that take different actions, and both u and A would be different for those that choose a value for x different from that chosen by other players. Thus, to analyze the possible existence and properties of asymmetric equilibria would require admitting the distribution of types as the aggregate state.

[8] In Sec. 4.2, we analyze the case when the output is measured by y^p.

Because ξ_t follows a normal distribution, ξ_t^2 follows the chi-squared distribution with the degree of freedom of one and g_t therefore follows a noncentral chi-squared distribution.[9] Since $\psi > 0$, the distribution of g_t is negatively skewed. The following corollary characterizes the first two moments of the growth distribution, including mean, median, variance and interquartile range (IQR).

Corollary 1 *In equilibrium, the distribution of growth g_{t+1} satisfies,*[10]

$$\begin{aligned} E\left(g_{t+1}\right) &= x - \psi C_{t+1} - \psi\left(1-\alpha^2\right)\tau \\ \mathbb{V}\left(g_{t+1}\right) &= 2\psi^2\left(1-\alpha^2\right)^2\tau^2 + \psi^2\left(\left(\alpha A_{t+1} - B_{t+1}\right)\alpha^t u_0\right)^2 \\ Median\left(g_{t+1}\right) &\approx x - \psi C_{t+1} - 0.47\psi\left(1-\alpha^2\right)\tau \\ IQR\left(g_{t+1}\right) &\approx \psi\left(1.22\left(1-\alpha^2\right)\tau + 1.34\left(\alpha A_t - B_t\right)\alpha^t u_0\right). \end{aligned}$$

If the parameter ratio $r \equiv \frac{\lambda}{\theta}$ satisfy $r > \left[2\left(1-\beta\right)-\left(1-\alpha\right)\right]\alpha^{-2}\left(1-\alpha\right)$, mean and median of the growth distribution are decreasing in uncertainty τ whereas the variance and IQR increase in uncertainty,

$$\frac{\partial E\left(g_{t+1}\right)}{\partial \tau} < 0,\ \frac{\partial Median\left(g_{t+1}\right)}{\partial \tau} < 0,\ \frac{\partial \mathbb{V}\left(g_{t+1}\right)}{\partial \tau} > 0,\ \frac{\partial IQR\left(g_{t+1}\right)}{\partial \tau} > 0.$$

As uncertainty rises, mean and median growth fall while the growth distribution becomes more dispersed. Intuitively, higher uncertainty raises the skill gap volatility. As a result, it becomes harder for Crusoe to predict "ideal" skill and it's more likely to generate a even larger foregone output due to the skill mismatch in the next period (i.e., higher chance of generating low growth). The future growth distribution therefore becomes more left-skewed.

However, we find this argument holds if and only if the penalty for skill mismatch λ is sufficiently large, i.e., under our parameter restriction $r \equiv \frac{\lambda}{\theta} > \left[2\left(1-\beta\right)-\left(1-\alpha\right)\right]\alpha^{-2}\left(1-\alpha\right)$ where α depends on r as shown in Eq. (10). In the limit when there is no penalty for skill mismatch, $\lambda \to 0$, growth increases in τ as the investment x rises. Figure 6 visually illustrates the parameter restrictions on r. The blue line plots $r - \left[2\left(1-\beta\right)-\left(1-\alpha\right)\right]\alpha^{-2}\left(1-\alpha\right)$ on r so that the E(g) decreases in uncertainty τ, i.e., $\frac{\partial E(g_{t+1})}{\partial \tau} < 0$, when the blue curve is above zero and the opposite holds otherwise. Thus, uncertainty is contractionary if the ratio of the penalty for skill mismatch λ over the cost of skill adjustment θ is 0.2% or higher. In Section 3.3, we estimate the model using monthly industrial production

[9] See details in https://mathworld.wolfram.com/NoncentralChi-SquaredDistribution.html

[10] The exact closed-form expression of quantiles of noncentral chi-squared distribution does not exist, we therefore use the approximation from Result 26.4.32 on page 942 of Abramowitz and Stegun (1948).

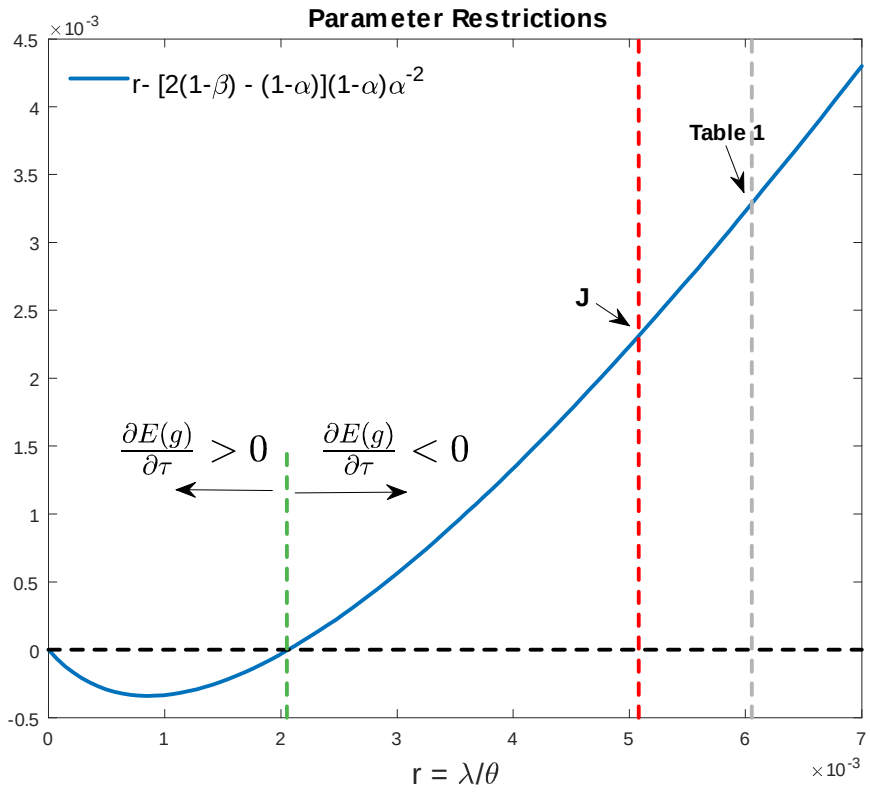

Figure 6: Parameter Restrictions for Uncertainty Impacts on Mean Growth. Note: the blue line portrarys $r - [2(1-\beta) - (1-\alpha)]\alpha^{-2}(1-\alpha)$ over $r = \lambda/\theta$. The red and grey dashed lines indicate the value of r used in Jovanovic (2006) and in Table 1 of the paper.

and find that this restriction holds (portrayed in dashed grey vertical line). Similarly, Jovanovic (2006) estimated the model using annual GDP per capita, and this restriction also holds (portrayed by point J on the dashed red vertical line).

In the long run as $t \to \infty$, the growth distribution doesn't depend on the initial values of u_0 and measures of centrality and dispersion of the growth distribution are bounded as long as u_t is stationary. The following corollary summarizes this finding.

Corollary 2 *When $t \to \infty$, the (long run) distribution of growth g_t does not depend on the initial condition u_0 and satisfies*

$$g_t = x - \psi x^2 \sigma^2 \xi_t^2 \tag{17}$$

The first two moments of the growth distribution are bounded in the limit and satisfy the

following expressions if and only if $\alpha < 1$,

$$\begin{aligned}
\lim_{t\to\infty} E(g) &= x - \psi\left(1-\alpha^2\right)\tau \\
\lim_{t\to\infty} \mathbb{V}(g) &= 2\psi^2\left(1-\alpha^2\right)^2\tau^2 \\
\lim_{t\to\infty} Median(g) &\approx x - 0.47\psi\left(1-\alpha^2\right)\tau \\
\lim_{t\to\infty} IQR(g) &\approx 1.22\psi\left(1-\alpha^2\right)\tau.
\end{aligned}$$

Growth-at-Risk (GaR).— Following Adrian et al. (2018), the Growth-at-Risk (GaR) at time t is defined as the lower 5th percentile of the growth distribution g_{t+1}. Because g_{t+1} follows a noncentral chi-squared distribution, its 5th percentile can be expressed approximately as

$$\chi_t \approx x - \psi C_{t+1} - 3.84\psi\left(1-\alpha^2\right)\tau - 1.65\psi\left(\alpha A_{t+1} - B_{t+1}\right)\alpha^t u_0. \tag{18}$$

In equilibrium, GaR decreases in uncertainty (τ),

$$\frac{\partial \chi_t}{\partial \tau} < 0.$$

Consistent with the empirical findings, larger uncertainty is associated with higher downside risk.

3.3 Impact of Uncertainty on Growth

Parameter choice.—The parameters are β, θ and λ. We cannot identify σ, λ,and θ separately, only $(\sigma\lambda, \sigma\theta)$. Therefore we set $\sigma = 1$. Table 1 reports the parameter estimates of the baseline model.[11]

Table 1 – Parameter Estimates

β	θ	λ
0.95	13,573	83

In order to capture the transitory impact of uncertainty as in the empirical section, we restrict parameters so that the uncertainty shock does not have a permanent effect on the distribution of the growth rate. More specifically, we set the discount rate at $\beta = 0.95$

[11] These estimates are similar to those in Jovanovic (2006, Table 1) which had $\lambda = 85$, $\theta = 16733$, where the model was estimated using GDP per capita, instead of industrial production.

and jointly estimate the parameters (λ, θ) to target the annualized long-run mean and standard deviation of the growth rate which are set to be 2% and 4.5%, respectively or,[12]

$$\begin{aligned} \lim_{t\to\infty} E\left(g_{t+1}\right) &= x - \psi x^2 = 2\%, \text{ and} \\ \lim_{t\to\infty} \sqrt{V\left(g_{t+1}\right)} &= \sqrt{2}\psi x^2 = 4.5\%. \end{aligned} \tag{19}$$

We now examine the impact of uncertainty on growth in the model. Starting with $\sigma = 1$, we change σ according to Eq. (14) to rise uncertainty τ by 15% and 30%, respectively, while adjusting (θ, λ) accordingly in each case to meet the target (19). In Sec. 4.1, by contrast, we shall introduce a two-state Markov process for σ and consider uncertainty shocks as occasional changes in σ while keeping (θ, λ) fixed. A 15% increase in uncertainty corresponds to a one-standard-deviation increase in JLN uncertainty.

We simulate the model for 60 periods and compute the changes in growth relative to the case when σ is fixed at 1. Figure 7 depicts the response of median growth in the top panel , interquartile range in the middle panel and 5th percentile (GaR) in the bottom panel to a unexpected increase in uncertainty at time 0. The blue line depicts the case with small uncertainty (15% increase in τ) while the red line reports results with large uncertainty (30% increase in τ). The dotted black line depicts the data counterpart reported in Figure 2. Similar to the empirical evidence, an increase in uncertainty is associated with lower median growth, higher interquartile range, and lower Growth-at-Risk. Quantitatively, our model suggests that one standard deviation increase in uncertainty immediately results in a 2% decline in median growth, a 2% increase in the growth dispersion and a 4% decline in GaR. Compared to the data, our model fits the impact response well but underpredicts (overpredicts) the median and GaR (interquartile range) in the long terms.[13] This suggests the effect of uncertainty is more persistent in the data.

Figure 8 depicts the response of various quantiles of the expected growth distribution to a 15% increase in uncertainty. Consistent with the empirical evidence reported in Figure 3, the response of the expected growth is highly nonlinear: an increase in uncertainty is associated with a larger decrease in the lower tail of the growth distribution whereas it has much smaller impact on the upper tail. Quantitatively, a 15% increase in uncertainty results in 3% decrease in 25th percentile of the expected growth distribution but only

[12] The targets are calculated as the historical mean and standard deviation of annual log differences in US industrial production from 1973:01 to 2018:12.

[13] One reason that the model doesn't match the empirical impulse responses well could be due to the nonparametric nature of local projections which are known to behave erratically at longer horizons in the conditional mean setting. See Barnichon and Brownlees (2019).

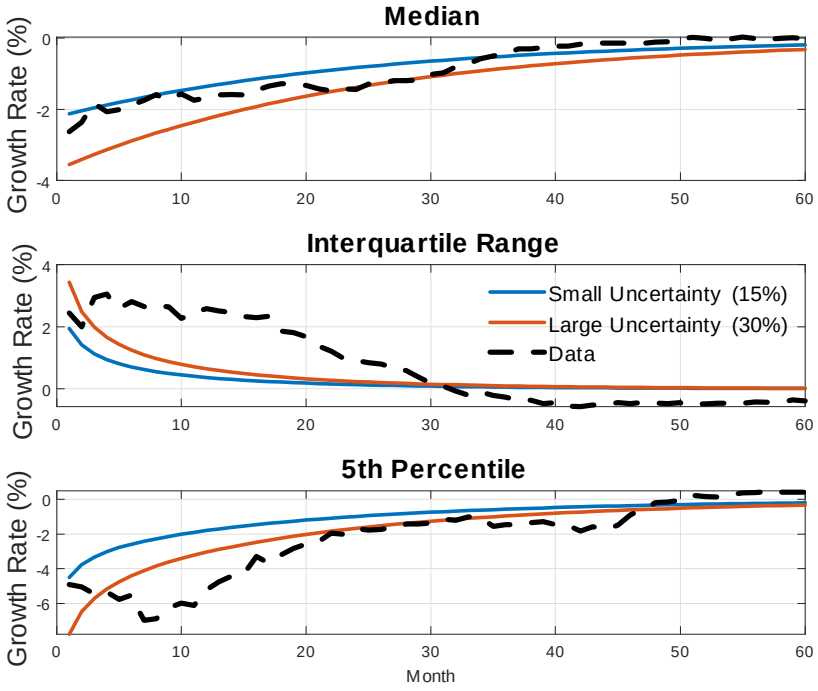

Figure 7: Uncertainty and Growth. Note: this figure depicts the response of median growth in the top panel , interquartile range in the middle panel and 5th percentile (GaR) in the bottom panel to an unexpected 15% (blue line) and 30% increase (red line) in uncertainty at time 0. The dashed black line is the empirical estimates from the baseline quantile regression described in the texts.

contributes to a 1% decline of the 75th percentile.

3.4 Occupational and job-to-job flows

One interpretation of h is that of organization capital in the sense of Prescott and Visscher (1980) in which a new technology has an unpredictable task-requirement coefficients. In that model labor is heterogeneous in its aptitude to perform the tasks well, and a realization of $x\varepsilon_{t+1}$ on the RHS of Eq. (13) would be interpreted as the change in the task requirements of the newly adopted technology, and this would call forth some adjustment of workers across tasks. With $x\varepsilon$ being identical across firms, the resulting adjustment of h would be purely internal to a firm, and could be seen as *occupational* switching by the firm's employees.

One can speculate on what the model would produce if, on the RHS of Eq. (13), ε_{t+1} was allowed to differ across firms. As a result, u_{t+1} would then also differ across firms and would imply a coexistence of heterogeneous technologies in a putty-clay framework.

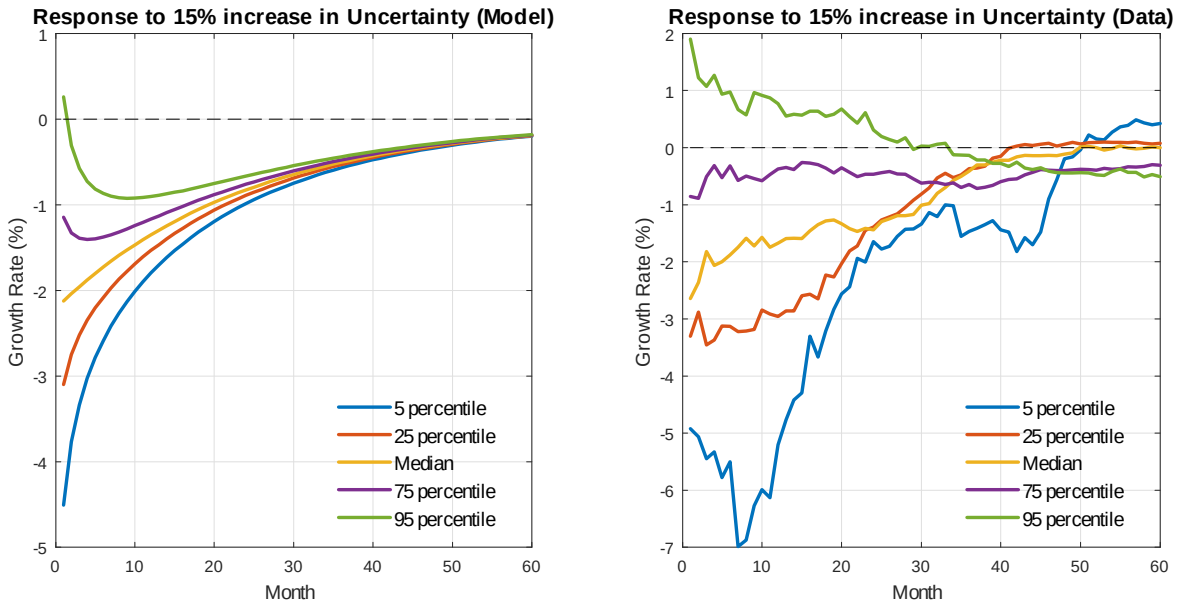

Figure 8: Asymmetric impact of uncertainty on growth. Note: the left panel depicts the response of various quantiles of the expected growth distribution to a 15% increase in uncertainty. The right panel reports the the empirical estimates from the baseline quantile regression described in the texts.

These include a labor market (Johansen (1959)) and firm-specific shocks to the cost of investment (Campbell (1998) and Gilchrist and Williams (2000)). These features would call forth for reallocation of labor among firms and would show up as job-to-job flows.

In sum, we shall think of occupational mobility and job-to-job mobility as proxies for the size of the skill gap, and uncertainty in these measures will be measured by the volatility of these measures. In this subsection, then, we empirically establish the connection between these two measures of labor reallocation – occupational and job-to-job mobility – and JLN macro uncertainty that is directly estimated by the volatility of the forecast errors of macro series.

We combine two data sources on labor mobility. The first data set is from Kambourov and Manovskii (2008); it reports occupational mobility at the 3-digit level between 1968 and 1997. We start the analysis in 1971, so as to match the start date of our uncertainty sample. The second data set is job-to-job mobility described in Hyatt, McEntarfer, McKinney, Tibbets and Walton (2014), which reports the sector-level job-to-job separation flows after 2000. We aggregated the job separations over all sectors.

For each measure, we compute its volatility as the 5-year rolling-window standard deviation. Figure 9 reports the scatterplot of these two measures of job mobility volatility

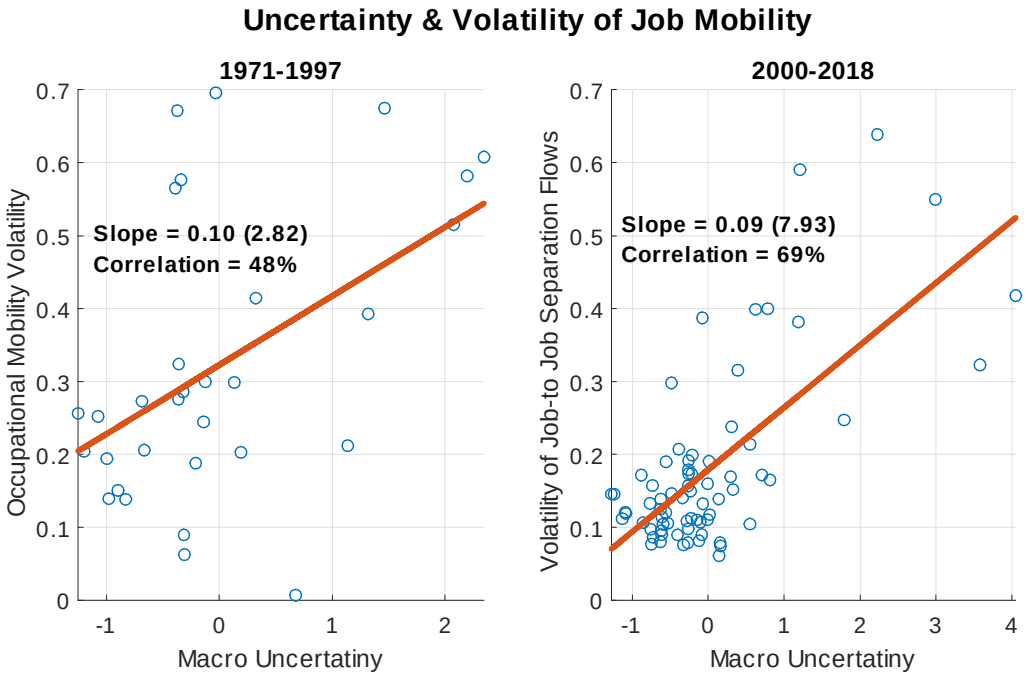

Figure 9: Uncertainty and volatility of occupational mobility. Note: this figure reports the scatterplot of the 5-year rolling-window volatility of the measure of occupational mobility from Kambourov and Manovskii (2008) against JLN macro uncertainty in the left panel. The right panel reports the scatter plot of 5-year rolling-window volatility of the job-to-job separation flow from Hyatt et al. (2014) against JLN macro uncertainty. In each panel, the OLS slope is reported, and the associated robust t-statistics are reported in parenthesis. The sample is annual for the left panel and is quarterly for the right panel.

against macro uncertainty. For both measures, JLN macro uncertainty and job mobility volatility are highly correlated, and we find a statistically significant positive relationship between the two. The right panel shows that JLN uncertainty is as high as 69% correlated with occupational mobility volatility, as measured by job-to-job separation flows. Results for pre-2000 sample using the occupation mobility measure are similar: despite a lower sample frequency for the pre-1997 sample, the JLN uncertainty is still 48% correlated with volatility of the occupational mobility from Kambourov and Manovskii (2008).

3.5 Capacity Utilization

King and Rebelo (1999) argue that capacity utilization combined with positive technology shocks yields utilization in generating realistic variation in output. This fits our model in which there never is technological regress because x is always positive. The model has no employed resources or spare capacity, but we may assume that the skill gap u_t is an

index of the fraction of capital – human or physical – that does not meet the needs of the date-t technology.

To do so, we return again to Prescott and Visscher (1980) whose model includes three tasks; two of the tasks are production tasks, while the third is a training task in which the firm is testing workers and trying to find out which of the two productive tasks a worker is better suited for. If adopting a new technology garbles some of the workers' task-specific abilities, then those workers would need to be re-tested and during the testing period would not be employed on productive tasks. The larger the technological leap x, the larger the fraction of workers whose abilities are garbled and then need re-testing. We may thus think of the workers being tested as spare capacity.

This interpretation of u_t would also be in the general spirit of Ljungqvist and Sargent (1988) explanation for high European unemployment in the last two decades of the 20th century in which higher unemployment reflected restructuring from manufacturing to services, adoption of new information technologies, and globalization. And since Klein and Su (1979) a number of studies show that capital and labor are utilized, by industries, at approximately the same rate in short run, implying a positive correlation at high frequencies between unemployment and spare capacity.

From equation (15), detrended output in the model depends on the skill gap u_t. While it's empirically challenging to directly estimate the skill gap in the data, the capacity utilization rate – the ratio of actual output to the potential output – can be used to test the relationship between u and growth. Monthly data on U.S. capacity utilization is available at the FRED economic data maintained by the St. Louis Fed (series id TCU). As before, we simulate the model using calibrated parameters reported in Table 1, and calculate skill gap u_t according to equation (13).[14] We define the capacity utilization as $1/|u_t|$ so that an increase in the skill gap leads to a fall in capacity utilization.

Figure 10 plots relation between model-implied Growth-at-Risk and the capacity utilization for the baseline model with $\sigma = 1$. Consistent with the data, the downside risk of the economy is much larger conditioning on small capacity utilization (i.e. large skill gap): a small changes in u_t can lead to *drastic* drop in growth-at-risk when capacity utilization is one standard deviation below its mean. Similar to what we will find with the VIX in the next subsection, our baseline model produces a better fit for the relation observed in the data than the OLS model.

[14] We consider the mean u_t at each t so that $u_t = \alpha^t u_0$.

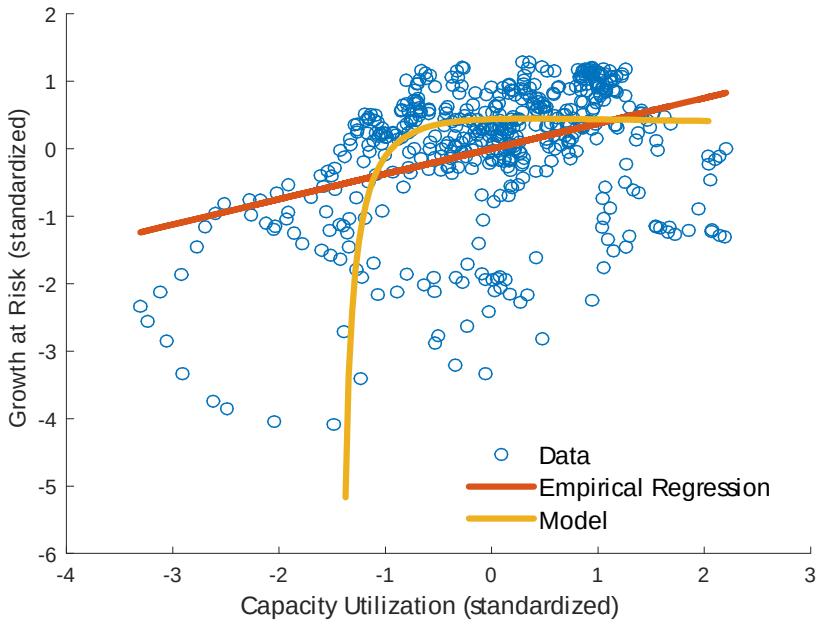

Figure 10: Capacity Utilization and Growth-at-Risk. Note: The red (yellow) reports model-generated contempraneous relationship between capacity utilization and Growth-at-Risk under OLS regression and our baseline model, respectively. Both series are standardized to have zero mean and unit variance. The blue dots depict the empirical counterpart.

3.6 Growth-at-Risk, the value of options and the VIX

For the price of a representative security $p(u, A)$ we have the Lucas (1978) equation

$$p(u, A) = \beta \int \frac{c(u, A)}{c(u', A + x)} \left[c(u', A + x) + p(u', A + x) \right] dF(\varepsilon), \tag{20}$$

where $u' = u + x\varepsilon - \Delta$. Although preferences being log, prices will fluctuate because consumption growth is autocorrelated. If low consumption today means high consumption growth, a disaster is accompanied by very low asset prices. A put option[15] is more valuable in such states, i.e., more likely to be "in the money." The opposite holds for call options. Therefore today's prices of those two derivative assets should be a good signal of Growth-at-Risk. Taking today's price as the strike price for both assets,

$$p^{\text{put}} = \int_{p(u', A+x) \leq p(u, A)} \left(p(u, A) - p(u', A + x) \right) dF(\varepsilon) \tag{21}$$

$$p^{\text{call}} = \int_{p(u', A+x) \geq p(u, A)} \left(p(u', A + x) - p(u, A) \right) dF(\varepsilon). \tag{22}$$

[15] From Investopedia: *A put option is an option contract giving the owner the right, but not the obligation, to sell a specified amount of an underlying security at a specified price within a specified time frame.*
.

The VIX index used in the empirical exercise contains put and call options on the individual firms in the S&P 500 index, and its price would reflect idiosyncratic as well as aggregate risk. The natural definition in our model is the sum of the prices of a call option and a put option with a strike price tomorrow equal to today's price of the security $p(u, A)$,

$$\text{VIX}(u, A) \equiv p^{\text{put}} + p^{\text{call}}. \tag{23}$$

We simulate the model and calculate the price the security from equation (20), and price of options and VIX according to equations (21) to (23) based on parameters reported in Table 1. The calculated VIX is further standardized to have zero mean and unit variance as in the empirical exercise.

Two series are plotted in Figure 11: the red line portrays data regression slope of GaR in the data on the VIX, while yellow lines depict model-generated VIX according equation (23) against GaR from equation (18). It shows that an increase in the VIX decreases the GaR in the model. This is consistent with the feature in the data that higher equity price volatility magnifies the negative impact of uncertainty on IP growth. Compared to a naive empirical linear regression, our model produces a better fit for the empirical relation between VIX and GaR.[16]

3.7 Long Run Growth Distribution

Based on equation (17), growth distribution follows a negative chi-squared distribution in the long run. The top panel of Figure 12 depicts the simulated long run distribution for different values of σ. We again use calibrated (λ, θ) such that the mean and variance of the long run distribution remain the same. It shows higher uncertainty leads to a more negatively skewed distribution (portrayed by red bars) and lower 5th percentile (red dashed line).

The chi-squared distribution is well known as a light-tailed distribution whereas in the traditional growth literature (e.g. Barro and Jin (2011)), the heavy-tailed distribution, such as the Pareto Distribution, has been commonly used to calculate the tail risk. To

[16]The baseline model produces a 38% smaller root-mean squared errors than OLS. The root-mean-squared error (RMSE) is defined as

$$RMSE = \sqrt{\frac{1}{T}\sum_{i=1}^{T}(\hat{y}_i - y_i)^2}$$

where the "hat" refers to the estimated value of GaR at time t. We find our model is able to outperform a quadratic regression model too.

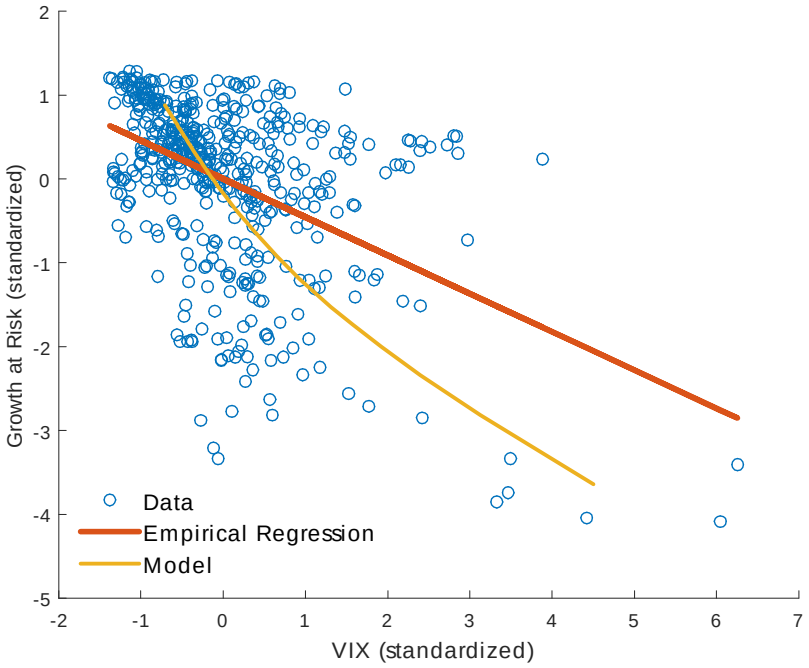

Figure 11: Asset Volatility and Growth-at-Risk. Note: The yellow (purple) reports model-generated contempraneous relationship between VIX and Growth-at-Risk under our baseline model and empirical OLS. The blue dots depict the empirical relationship. Both VIX and GaR are standardized to have zero mean and unit variance. The red line reports the OLS Estimate.

address this issue, we assume that in the long horizon, the growth distribution follows,

$$g_t = x - \psi x^2 \sigma^2 z_t.$$

The variable $z_t \in [0, \infty)$ follows a Type-II Pareto Distribution with associated CDF,

$$F(z_t) = 1 - (1 + x)^{-\alpha},$$

where α is the shape parameter that governs the tail thickness.

We randomly draw 10,000 z_t from $F(z_t)$ and numerically calculate α by targeting the lower 5th percentile to be the corresponding value in the calibrated Chi-squared distribution with $\sigma^2 = 1$. The bottom panel of Figure 12 depicts the simulated growth distribution using Pareto distribution with $\alpha = 2.83$ (in red bars) against the baseline growth distribution with chi-squared distribution. It shows that Pareto distribution has a thicker tail than the Chi-squared distribution. Therefore, in order to generate the same downside risk, measured by the lower 5th percentile, the growth distribution with Pareto has much smaller mean growth (0.78%) than the chi-squared distribution (1.50%).

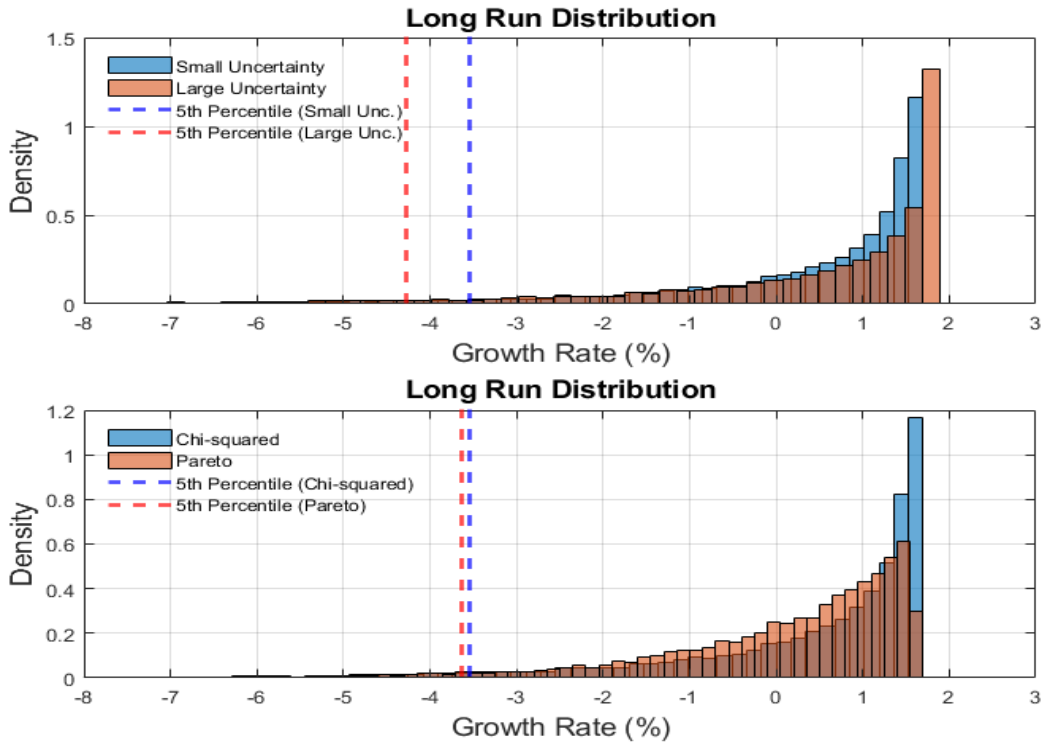

Figure 12: Simulated Long-run Growth Distribution. Note: the upper panel shows the simulated long-run growth distribution for small uncertainty (blue bars) and large uncertainty (red bars). The lower panel shows the simulated long-run growth distribution with Pareto distribution (red bars) and Chi-squared distribution (blue bars).

3.8 Technological commitment

It's worth noting that the assumption of irreversible technological commitment is essential to generate the negatively skewed growth distribution in equilibrium: output could fall because of commitment to technology before an unfavorable shock ε is realized. If a firm could revert quickly and costlessly to technologies it used before, it would *always* use the best technology up to date and output never declines. For example, Jovanovic and Rob (1990) assume costless recall of past technologies.[17] In contrast to our empirical evidence, instead of having a left tail, the distribution of growth rates in their model exhibits a spike at zero and a *right* tail. Therefore, we need at least partial technological commitment.

[17]Recent related papers include Bardhi (2019) and Wong (2020).

4 Extensions of the model

The following subsections present three extensions. Sec. 4.1 considers a two-state Markov process for σ; so far, to derive the impact of uncertainty on growth, Sec. 3 starts with $\sigma = 1$ and then lowers it to 0.95 and 0.87, interpreting the change in σ as permanent and completely unexpected. Here, as in Bloom (2009), we shall model σ as a shock that follows a two-state Markov process the parameters of which the agents understand. Predictably, growth is slower when uncertainty is high but Δ is state independent, and it is the same as it was in the constant-σ case.

Sec. 4.2 changes the definition of measured output. So far we assumed that output, y, was *net* output, which is potential output minus the adjustment cost of production. One may ask whether this is the reasonable counterpart to the data, and how the results change if we use y^p instead of y. It turns out, however, that the theoretical predictions are virtually the same due to the presence of foregone output from the skill gap.

Finally, Sec. 4.3 analyzes Epstein-Zin preferences; the model so far used log preferences which are not ideal for explaining stock-price movements and the equity premium puzzle. This seems relevant when analyzing the VIX. We indeed find that our model under recursive preferences is able to produce the same predictions from the baseline model under standard choices of preference parameters while generating a more realistic VIX.

4.1 A two-state Markov process for σ

Instead of comparing long run growth for two different values of σ, we now follow Bloom (2009, Eqs. 3.5 and 3.6) and imagine a two state symmetric Markov process for $\sigma \in \{\sigma_{\mathrm{L}}, \sigma_{\mathrm{H}}\}$ with transition probabilities $p_{i,j}$ between the states $i, j \in \{\mathrm{L}, \mathrm{H}\}$. This allows us to study the effects of uncertainty shifts that are that agents expected to be temporary (unless $p_{i,i} = 1$).[18]

The Bellman equation (7) now acquires a new state $i \in \{\mathrm{L}, \mathrm{H}\}$:

$$V_i(u, A) = \max_{x,\Delta} \left\{ \ln y(u, \Delta, A) + \beta \int \left(\sum_j p_{i,j} V_j(u + x\varepsilon - \Delta, A + x) \right) dF\left(\frac{\varepsilon}{\sigma_i}\right) \right\}. \tag{24}$$

Assume symmetry of the process so that $p_{i,i} = p_{j,j} = p$. In an abbreviated form Eq. (24) then reads

$$V_i = \max_{x,\Delta} \left\{ \ln y + \beta \int \left(pV_i' + (1-p) V_j' \right) dF_{\mathrm{i}} \right\}, \tag{25}$$

[18] Other related papers are Gourio (2012), Gabaix (2012), and Wachter (2013).

where $F_i = F\left(\frac{\varepsilon}{\sigma_i}\right)$, and where primes denote next period values of a variable.

The optimal policies are the same as in the constant-σ case: The effect on x of a temporary reduction in σ is identical to its effect in Eq. (8) where it is assumed to be permanent:

Proposition 3 *The optimal x is state-dependent; for $i \in \{L, H\}$ we have*

$$x_i = \frac{1}{\theta\sigma_i^2 (1-\beta)(1-\alpha)}. \tag{26}$$

The optimal Δ does not depend on the state, and is the same as in the constant-σ case:

$$\Delta_L = \Delta_H = (1-\alpha)\, u, \tag{27}$$

where α remains the same as constant-σ case and is expressed by (10).

The proof is in Appendix 3. Proposition 3 also shows that the adjustment Δ indicating the fraction of the skill gap that the agent closes is the same the one from as constant-σ case. As a result, the agent chooses the same amount of investment in skills, whether σ is expected to be changed or not in the future.[19]

Proposition 1 is a special case that obtains when $p = 1$ or, equivalently, when $\sigma_{\mathrm{L}} = \sigma_{\mathrm{H}}$. Similar to the case where σ_i is fixed over time, the conditional growth distribution g_i is a linear combination of a normal distribution and a chi-squared. We summarize our key findings in the following corollary also proved in Appendix 3:

Corollary 3 *At state $i \in \{L, H\}$ growth equals*

$$g_i = \left[x_i + \psi\left(1-\alpha^2\right)u^2\right] + 2\psi\alpha u x_i \sigma_i \xi - \psi x_i^2 \sigma_i^2 \xi^2. \tag{28}$$

where

$$\xi \sim N(0,1) \qquad \textit{and} \qquad \psi = \frac{1}{2}\left(\lambda\alpha^2 + \theta(1-\alpha)^2\right)$$

Conditional on u, the distribution of growth g a is left skewed and its mean and skewness satisfy

$$\begin{aligned} E(g_i|u) &= x_i + \psi\left(1-\alpha^2\right)u^2 - \psi\tau_i \\ \mathit{Skewness}(g_i|u) &= -2.82\psi\left(1-\alpha^2\right)\tau_i < 0 \end{aligned} \tag{29}$$

where the uncertainty at state i satisfies

$$\tau_i \equiv var(u) = \frac{x_i^2\sigma^2}{1-\alpha^2} = \left((1-\beta)^2\left(1-\alpha^2\right)\theta^2(1-\alpha)^2\right)^{-1}\sigma_i^{-2}. \tag{30}$$

[19] This is due to the assumption of log utility. Section 4.3 shall show that under a more general recursive preferences, α varies with current skill gap u, instead of being a constant.

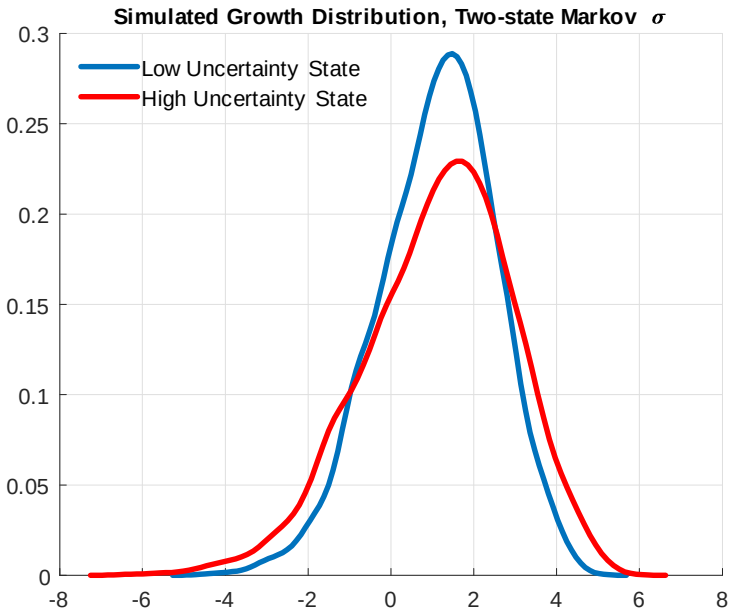

Figure 13: Conditional growth distribution. Note: this figure plots the simulated growth distribution for $\sigma = 0.95$ (blue line) and $\sigma = 0.87$ (red line) conditional on $u = 1$. We draw 5000 ξ randomly from the standard normal distribution, and generate g_L and g_H according to Eq.(28).

Equation (29) shows that the higher uncertainty τ_i induces a more negative-skewed distribution in equilibrium; and according to equation (30), state with high uncertainty corresponds to the state with low σ_i. Fig. 13 depicts the simulated distribution under low uncertainty state where we set $\sigma_L = 0.95$ and high uncertainty state where we set $\sigma_H = 0.87$, conditional on $u = 1$. We draw 5,000 ξ randomly from standard normal distribution, and generate g_L and g_H according to Eq. 28. The red line shows the simulated conditional PDF of g_H conditional on $u = 1$ and the blue line shows the counterpart PDF of g_L. As shown in the figure, higher uncertainty induces a more negatively-skewed distribution and the distribution under the red curve exhibits a fatter left tail than the blue curve.

While we have shown analytically that state with higher uncertainty is associated with a more left-skewed conditional growth distribution, it is still of interest to study impact of the uncertainty on the *unconditional* growth distribution. While there is no closed-form solution to the unconditional growth distribution, we simulate the model for $T = 10$ periods and calculate the evolution of the growth distribution. More specifically, we start with $u_0 = 1$ and $\sigma_0 = \sigma_L = 0.95$. For each $t = 1, 2..., T$, we draw 5000 ξ randomly from standard normal distribution and calculate the growth distribution according to Eq. 28 according to the state at time t. The state stays unchanged, i.e. $\sigma_t = \sigma_{t-1}$, with

probability p and u_{t+1} is updated according to equation (13).

We set $p = 0.71$ following Bloom (2009b) so that the half-life of an uncertainty shock on average is 2 months. We are thus looking at short-run changes in uncertainty. Figure 14 depicts the simulated distribution for $t = 1, 4, 10$. The top panel of the figure shows that the simulated economy is changed from the low uncertainty state to the high uncertainty state at $t = 4$. As a result, compared to the growth distribution at $t = 1$ (blue curve), the growth distribution at the time of the uncertainty shock (red curve) immediately becomes more dispersed and more negatively skewed. From time $t = 5, 6..., 10$ sans uncertainty shock, the growth distribution becomes less and less negatively skewed as the average skill gap u decreases.

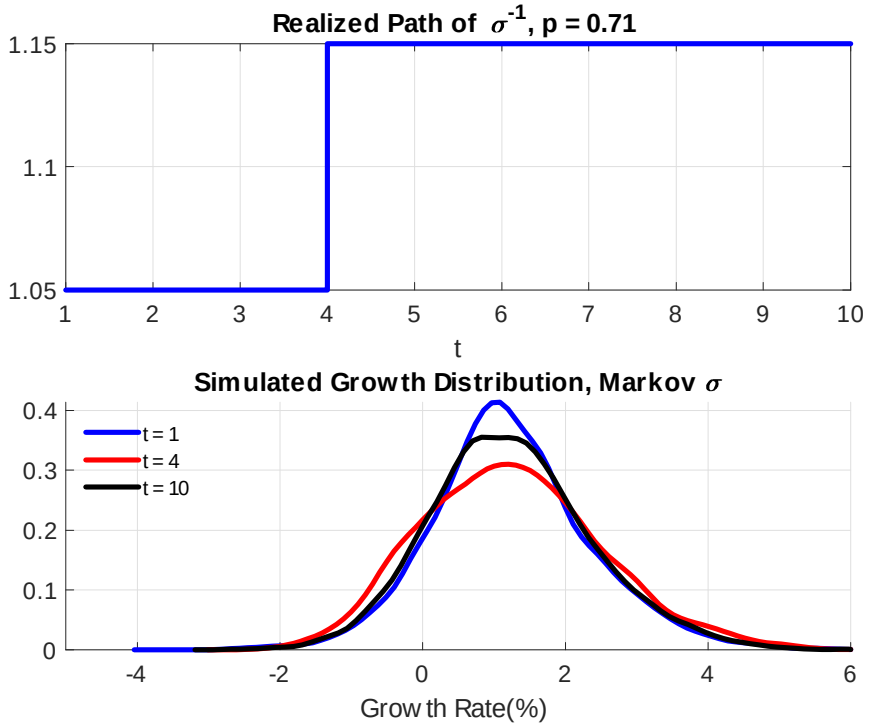

Figure 14: Simulated growth distribution. Note: this figure plots the simulated evolution of σ (top panel) and the growth distribution (bottom panel) at time 1, 4, and 10 when the economy starts at $u = 1$ and $\sigma = 0.95$. For each time t, we draw 5000 ξ randomly from the standard normal distribution, and generate g_L and g_H according to Eq. (28).

Thus the findings in Sec. 3 that were based on the constant-σ model and related to permanent changes in σ, still hold up here in the sense that the rise in uncertainty at date 4, now perceived to be fairly temporary, still leads to a thicker lower tail of the growth distribution and to a much smaller impact on its upper tail.

4.2 Potential output versus net output

In our baseline model, forgone output $C(y^p, \Delta)$ captures the cost of adjustment of skill h. The closeness of u to zero can be viewed as a form of intangible capital. Rapid adjustment of technology causes this intangible capital to depreciate, and $C(y^p, \Delta)$ can be interpreted as *unmeasured* investment.[20]

We now show that our analytical results on the impact of uncertainty are not driven by the presence of $C(y^p, \Delta)$; the model's implications remain qualitatively the same when potential output, instead of net output, is used to measure the economic growth.

First, according to Eqs. (3) and (5), potential output y^p can be expressed as

$$\begin{aligned} y^p &= \exp\left\{A - \frac{\lambda}{2}(u-\Delta)^2\right\} \\ &= y\exp\left\{\frac{\theta}{2}(1-\alpha)^2 u^2\right\} \end{aligned}$$

Then the log of potential output is

$$\begin{aligned} \ln y_t^p &= \ln y_t + \frac{\theta}{2}(1-\alpha)^2 u^2 \\ &= A_0 + xt - \frac{\lambda}{2}\alpha^2 u_t^2, \end{aligned}$$

where the second line follows from equation (15) and equation (12). Then the growth of y^p can be expressed as

$$g_{t+1}^p \equiv \ln y_{t+1}^p - \ln y_t^p = x - \frac{\lambda}{2}\alpha^2\left(u_{t+1}^2 - u_t^2\right),$$

and the following result is proved in the Appendix 4:

Proposition 4 *Conditional on initial output and technology level y_0^p and A_0, if ε_t follows a normal distribution $N(0,\sigma^2)$, the distribution of growth g_t^p is left-skewed and expressed as*

$$g_t^p = x - \frac{\lambda}{2}\alpha^2\left[C_t + \left(1-\alpha^2\right)\tau\xi_t^2 + \left(\alpha A_t - B_t\right)\alpha^t u_0^p \xi_t\right],$$

where $\xi_t \sim N(0,1)$ follows standard normal distribution and A_t, B_t, and C_t are the same as in proposition 2, and

$$u_0^p = \sqrt{\frac{2}{\lambda\alpha^2}\left(ln y_0^p - A_0\right)^2}.$$

[20] McGrattan and Prescott (2014) and Bhandari and McGrattan (2018) use data from U.S. national accounts and business census data and estimate a ratio of intangible to total assets in private business that is close to 60 percent, and that intangible are especially large for high-technology sectors that have important input-output linkages with other sectors. Table 2 of Chappell and Jaffe (2018) reports results for New Zealand.

Therefore, similar to the net output, the distribution of the total output growth g_t^p is also left-skewed and the following corollary suggests that our results remain the same qualitatively if total output is used.

Corollary 4 *In equilibrium, the moments of distribution of growth g^p and the growth-at-risk χ^p satisfy,*

$$\frac{\partial E\left(g_{t+1}^p\right)}{\partial \tau} < 0, \frac{\partial Median\left(g_{t+1}^p\right)}{\partial \tau} < 0, \frac{\partial \mathbb{V}\left(g_{t+1}^p\right)}{\partial \tau} > 0, \frac{\partial IQR\left(g_{t+1}^p\right)}{\partial \tau} > 0, \frac{\partial \chi^p}{\partial \tau} < 0$$

4.3 Recursive Preferences

The model so far used log preferences for analytical tractability. However, this assumption generates counterfactual stock-price movements (i.e. the equity premium puzzle). In this section, we extend the model using Epstein and Zin (2013) recursive preferences. The Bellman equation (7) now becomes

$$V_{EZ}(u, A) = \max_{x,\Delta} \left[y(u, \Delta, A)^{1-\phi} + \beta \left[\int V_{EZ}(u + x\varepsilon - \Delta, A + x)^{1-\gamma} dF\left(\frac{\varepsilon}{\sigma}\right) \right]^{\frac{1-\phi}{1-\gamma}} \right]^{\frac{1}{1-\phi}} \tag{31}$$

where $y(u, \Delta, A) = \exp\left\{A - \frac{\lambda}{2}(u - \Delta)^2 - \frac{\theta}{2}\Delta^2\right\}$, γ is the risk aversion coefficient, and the parameter ϕ is the inverse of the elasticity of substitution (IES).

Because recursive preferences are homothetic, the following proposition shows that the optimal investments (x, Δ) are independent of the productivity A.

Proposition 5 *The value function can be expressed as*

$$V_{EZ}(u, A) = e^A v(u)$$

and x and Δ are independent of A.

While there are no general closed-form solutions to $V_{EZ}(u, A)$ for all pairs (γ, ϕ), the following corollary shows that in a special case where $\gamma = \phi = 1$, the log of the EZ value function satisfies equation (11).

Corollary 5 *When $\gamma = \phi = 1$,*

$$lnV_{EZ}(u, A) = \frac{A}{1 - \beta} - \frac{1}{2}\theta(1 - \alpha)u^2 + J$$

where J satisfies equation (12).

Parameter choice.— The parameters of this extended model are $\beta, \gamma, \phi, \lambda$ and θ. Table 2 reports the parameter estimates.

Table 2 – Parameters Estimates under Recursive Preferences

β	γ	ϕ	λ	θ
0.95	5	0.95^{-1}	8	21

To solve the model, we follow the baseline model and set parameters (λ, θ) to target the long-run mean and standard deviations of the growth rate valued at 2% and 4.5%, respectively. For other parameters, we set the risk aversion parameter to be $\gamma = 5$, and set $1/\phi$, the elasticity of intertemporal substitution (IES), to be 0.95, which is in line with macro studies such as Hall (1988). As in the baseline model, we express the optimal skill investment in terms of $\alpha_{EZ}(u)$ so that $\Delta_{EZ}(u) = [1 - \alpha_{EZ}(u)]\, u$, and numerically calculate the policy functions $(x_{EZ}(u), \alpha_{EZ}(u))$ based on the numerical procedure described in the Appendix.

Figure (15) shows the optimal $x_{EZ}(u)$ and $\alpha_{EZ}(u)$. Different from the baseline model featuring log utility where x and α are *constant*, optimal investment decisions $x_{EZ}(u)$ and $\alpha_{EZ}(u)$ under recursive preferences now vary with the skill gap u. Under the current parametrization, the investment in technology x declines as the skill gap rises while the fraction of skill gap invested in skill, $1 - \alpha_{EZ}$, increases in u.

Turning to the growth, the log of measured output satisfies,

$$\begin{aligned} \ln y_t &= A - \frac{\lambda}{2}\alpha_{EZ}^2 u_t^2 - \frac{\theta}{2}(1 - \alpha_{EZ})^2 u_t^2 \\ &= A_0 + \sum_{s=1}^{t} x_{EZ,s} - \psi_{EZ,t} u_t^2, \end{aligned}$$

where $\psi_{EZ,t} \equiv \frac{1}{2}\left[\lambda \alpha_{EZ,t}^2 + \theta (1 - \alpha_{EZ,t})^2\right]$. Therefore, the log growth can be expressed as,

$$g_{t+1} \equiv \ln y_{t+1} - \ln y_t = x_{EZ,t+1} - \psi_{EZ,t+1} u_{t+1}^2 + \psi_{EZ,t} u_t^2. \tag{32}$$

where the skill gap follows $u_{t+1} = \alpha_{EZ} u_t + x_{EZ,t+1}\sigma\xi_{t+1}$. While there is no closed-form solution to the growth distribution (32) under recursive preferences, we start with $u_0 = 1$ and simulate the model for $T = 10$ periods using the parameterization for Figure (15). For each $t = 1, 2..., T$, we draw 5000 ξ randomly from standard normal distribution and calculate the growth distribution according to Eq. 32 for low uncertainty where we set $\sigma = 0.95$ and high uncertainty where we set $\sigma = 0.87$.

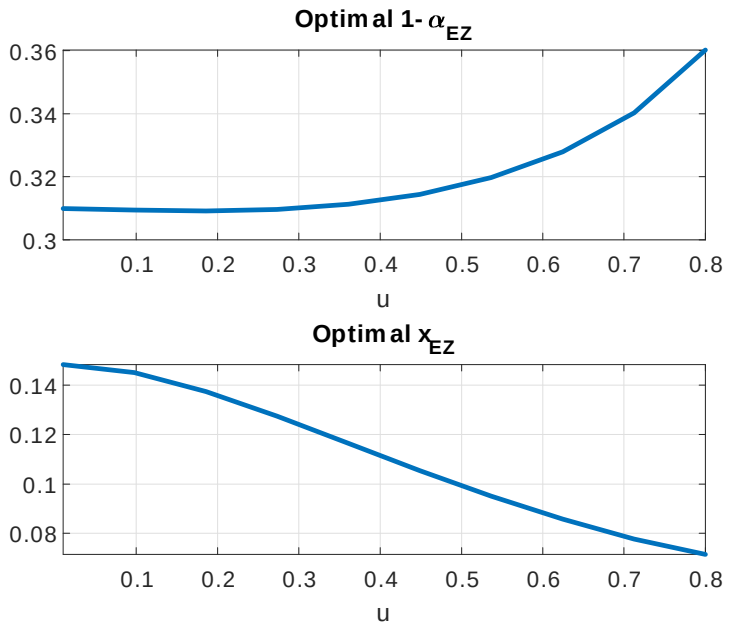

Figure 15: Policy Functions under Recursive Preferences. Note: this figure plots the optimal policy function x and α under recursive preferences over the grid of skill gap u. See texts for the parameter choices.

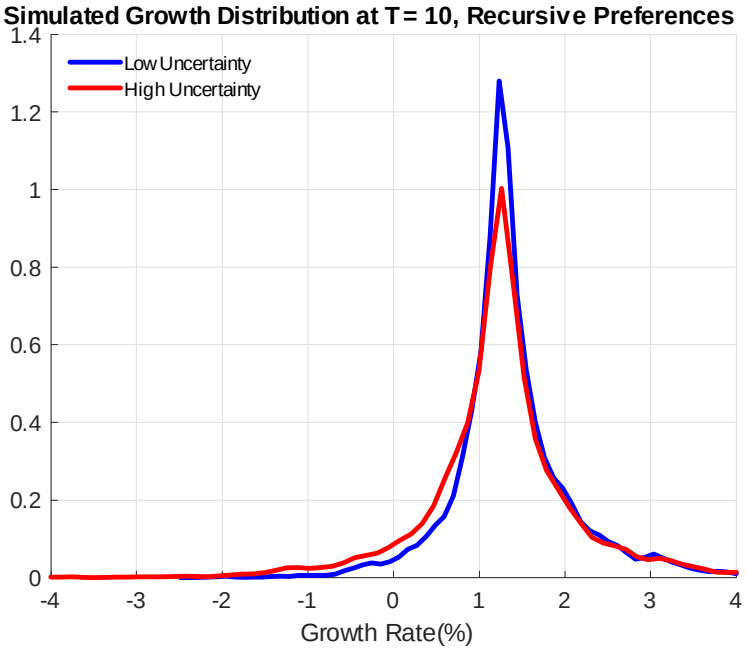

Figure 16: Simulated growth distribution under Recursive Preferences. Note: this figure plots the simulated growth distribution time 10 when the economy starts at $u = 1$. For each time t, we draw 5000 ξ randomly from the standard normal distribution, and generate g according to Eq. (32) under high and low uncertainty, respectively.

Figure 16 plots the simulated growth distribution at time $T = 10$. Similar to the baseline model, the growth distribution is negatively skewed. Compared to the distribution under low uncertainty (portrayed by the blue curve), high uncertainty (portrayed by the red curve) induces a more dispersed and more negative skewed growth distribution.

Asset Pricing.— For the price of a representative security $p(u, A)$, the Lucas (1978) equation (20) now becomes

$$p(u, A) = \beta \int M(u, A) \left[c(u', A + x) + p(u', A + x) \right] dF\left(\frac{\varepsilon}{\sigma}\right),$$

where the stochastic discount factor satisfies,

$$M(u, A) = \left(\frac{y(u', A + x)}{y(u, A)} \right)^{-\phi} \left(\frac{V_{EZ}(u + x\varepsilon - \Delta, A + x)^{1-\gamma}}{\int V_{EZ}(u + x\varepsilon - \Delta, A + x)^{1-\gamma} dF\left(\frac{\varepsilon}{\sigma}\right)} \right)^{\phi-\gamma}.$$

The model's VIX can be then calculated based on equation (23). We use the same parameterization for Figure (15) and simulate the model for $T = 508$ periods, which corresponds to the sample size of our empirical exercise. The model's VIX is further normalized to have zero mean and unit variance over the simulation sample.

We find that the more general recursive preferences improve model's fit to the data. The correlation between the model implied VIX and the data is 31%, increasing from 18% under log utility. In short, our model under recursive preferences is able to generate the same implications from the baseline model while matching the mean and variance of long-run growth and generating more realistic VIX under standard choices of preference parameters (γ, ϕ) from macro literature.

5 Conclusion

In this paper, we documented several stylized facts on the real effects of uncertainty. First, we showed that higher economic uncertainty is closely associated with a more dispersed growth distribution. Second, we found that the response of IP growth to an increase in uncertainty is highly nonlinear and asymmetric. Third, we presented evidence that higher asset volatility magnifies the negative impact of uncertainty on growth.

We then presented and estimated a model in which growth and uncertainty are both endogenous. Rapid adoption of new technology leads in equilibrium to higher economic uncertainty that may cause measured productivity to decline for a while. The model matches several key features in the data. The equilibrium growth distribution is negatively skewed and higher uncertainty leads to higher downside risk, and to more labor

reallocation among jobs and among occupations. The model also generates a negative nonlinear relation between asset price volatility and Growth-at-Risk, as observed in the data.

References

Abramowitz, Milton and Irene A Stegun, *Handbook of mathematical functions with formulas, graphs, and mathematical tables*, Vol. 55, US Government printing office, 1948.

Adrian, Tobias, Federico Grinberg, Nellie Liang, and Sheheryar Malik, *The term structure of growth-at-risk*, International Monetary Fund, 2018.

___ **, Nina Boyarchenko, and Domenico Giannone**, "Vulnerable growth," *American Economic Review*, 2019, *109* (4), 1263–89.

Alfaro, Ivan, Nicholas Bloom, and Xiaoji Lin, "The Real and Financial Impact of Uncertainty Shocks," in "Stanford Institute for Theoretical Economics (SITE) 2016 Workshop. Retrieved from https://site. stanford. edu/sites/default/files/alfaro. pdf" 2016.

Angelini, Giovanni, Emanuele Bacchiocchi, Giovanni Caggiano, and Luca Fanelli, "Uncertainty across volatility regimes," *Journal of Applied Econometrics*, 2019.

Arellano, Cristina, Yan Bai, and Patrick Kehoe, "Financial Markets and Fluctuations in Uncertainty," January 2011. Federal Reserve Bank of Minneapolis Research Department Staff Report 466.

Baker, Scott R and Nicholas Bloom, "Does uncertainty reduce growth? Using disasters as natural experiments," Technical Report, National Bureau of Economic Research 2013.

___ **,** ___ **, and Steven J Davis**, "Measuring economic policy uncertainty," *The Quarterly Journal of Economics*, 2016, *131* (4), 1593–1636.

Bardhi, Arjada, "Evaluation and Influence through Selective Learning of Attributes," *Available at SSRN 3468546*, 2019.

Barnichon, Regis and Christian Brownlees, "Impulse response estimation by smooth local projections," *Review of Economics and Statistics*, 2019, *101* (3), 522–530.

Barro, Robert J and Tao Jin, "On the size distribution of macroeconomic disasters," *Econometrica*, 2011, *79* (5), 1567–1589.

Basu, Susanto and Brent Bundick, "Uncertainty shocks in a model of effective demand," *Econometrica*, 2017, *85* (3), 937–958.

Berger, David, Ian Dew-Becker, and Stefano Giglio, "Uncertainty shocks as second-moment news shocks," *The Review of Economic Studies*, 2020, *87* (1), 40–76.

Bernanke, Ben S., "Irreversibility, Uncertainty, and Cyclical Investment," *The Quarterly Journal of Economics*, 1983, *98* (1), 85–106.

Bhandari, Anmol and Ellen R McGrattan, "Sweat equity in US private business," Technical Report, National Bureau of Economic Research 2018.

Bianchi, Francesco, Cosmin L Ilut, and Martin Schneider, "Uncertainty shocks, asset supply and pricing over the business cycle," *The Review of Economic Studies*, 2017, *85* (2), 810–854.

____ , Howard Kung, and Mikhail Tirskikh, "The origins and effects of macroeconomic uncertainty," Technical Report, National Bureau of Economic Research 2018.

Bloom, Nicholas, "The Impact of Uncertainty Shocks," *Econometrica*, May 2009, *77* (3), 623–85.

____ , "The impact of uncertainty shocks," *econometrica*, 2009, *77* (3), 623–685.

____ , Max Floetotto, Nir Jaimovich, Itay Saporta-Eksten, and Stephen J Terry, "Really uncertain business cycles," *Econometrica*, 2018, *86* (3), 1031–1065.

Bolton, Patrick and Christopher Harris, "Strategic experimentation," *Econometrica*, 1999, *67* (2), 349–374.

Caldara, Dario, Cristina Fuentes-Albero, Simon Gilchrist, and Egon Zakrajšek, "The macroeconomic impact of financial and uncertainty shocks," *European Economic Review*, 2016, *88*, 185–207.

Campbell, Jeffrey R, "Entry, exit, embodied technology, and business cycles," *Review of economic dynamics*, 1998, *1* (2), 371–408.

Carriero, Andrea, Todd E Clark, and Massimiliano Marcellino, "Measuring uncertainty and its impact on the economy," *Review of Economics and Statistics*, 2018, *100* (5), 799–815.

Chalkley, Martin and In Ho Lee, "Learning and asymmetric business cycles," *Review of Economic Dynamics*, 1998, *1* (3), 623–645.

Chappell, Nathan and Adam Jaffe, "Intangible investment and firm performance," *Review of Industrial Organization*, 2018, *52* (4), 509–559.

Dew-Becker, Ian, Alireza Tahbaz-Salehi, and Andrea Vedolin, "Skewness and time-varying second moments in a nonlinear production network: theory and evidence," 2020.

Epstein, Larry G and Stanley E Zin, "Substitution, risk aversion and the temporal behavior of consumption and asset returns: A theoretical framework," in "Handbook of the fundamentals of financial decision making: Part i," World Scientific, 2013, pp. 207–239.

Fajgelbaum, Pablo D, Edouard Schaal, and Mathieu Taschereau-Dumouchel, "Uncertainty traps," *The Quarterly Journal of Economics*, 2017, *132* (4), 1641–1692.

Fernández-Villaverde, Jesús, Juan F. Rubio-Ramírez Pablo Guerrón-Quintana, and Martin Uribe, "Risk Matters: The Real Effects of Volatility Shocks," *American Economic Review*, October 2011, *6* (101), 2530–61.

Gabaix, Xavier, "Variable rare disasters: An exactly solved framework for ten puzzles in macro-finance," *The Quarterly journal of economics*, 2012, *127* (2), 645–700.

Gilchrist, Simon and John C Williams, "Putty-clay and investment: a business cycle analysis," *Journal of Political Economy*, 2000, *108* (5), 928–960.

___ , Jae W. Sim, and Egon Zakrajsek, "Uncertainty, Financial Frictions, and Investment Dynamics," June 2010. Society for Economic Dynamics 2010 Meeting Papers No.1285.

Gourio, Francois, "Disaster risk and business cycles," *American Economic Review*, 2012, *102* (6), 2734–66.

Gulen, Huseyin and Mihai Ion, "Policy uncertainty and corporate investment," *The Review of Financial Studies*, 2016, *29* (3), 523–564.

Hall, Robert E, "Intertemporal substitution in consumption," *Journal of political economy*, 1988, *96* (2), 339–357.

Hengge, Martina, "Uncertainty as a Predictor of Economic Activity," 2019.

Hyatt, Henry R, Erika McEntarfer, Kevin L McKinney, Stephen Tibbets, and Doug Walton, "Job-to-job (J2J) flows: New labor market statistics from linked employer-employee data," *US Census Bureau Center for Economic Studies Paper No. CES-WP-14-34*, 2014.

Johansen, Leif, "Substitution versus fixed production coefficients in the theory of economic growth: a synthesis," *Econometrica: Journal of the Econometric Society*, 1959, pp. 157–176.

Jordà, Òscar, "Estimation and inference of impulse responses by local projections," *American economic review*, 2005, *95* (1), 161–182.

Jovanovic, Boyan, "Asymmetric cycles," *The Review of Economic Studies*, 2006, *73* (1), 145–162.

—— **and Rafael Rob**, "Long waves and short waves: Growth through intensive and extensive search," *Econometrica: Journal of the Econometric Society*, 1990, pp. 1391–1409.

Jurado, Kyle, Sydney C. Ludvigson, and Serena Ng, "Measuring Uncertainty," *The American Economic Review*, 2015, *105* (3), 117–1216.

Kambourov, Gueorgui and Iourii Manovskii, "Rising occupational and industry mobility in the United States: 1968–97," *International Economic Review*, 2008, *49* (1), 41–79.

Keller, Godfrey, Sven Rady, and Martin Cripps, "Strategic experimentation with exponential bandits," *Econometrica*, 2005, *73* (1), 39–68.

King, Robert G and Sergio T Rebelo, "Resuscitating real business cycles," *Handbook of macroeconomics*, 1999, *1*, 927–1007.

Klein, Lawrence R and Vincent Su, "Direct estimates of unemployment rate and capacity utilization in macroeconometric models," *International Economic Review*, 1979, pp. 725–740.

Klenow, Peter J, "Learning curves and the cyclical behavior of manufacturing industries," *Review of Economic dynamics*, 1998, *1* (2), 531–550.

Leduc, Sylvain and Zheng Liu, "Uncertainty shocks are aggregate demand shocks," *Journal of Monetary Economics*, 2016, *82*, 20–35.

Ljungqvist, L and T Sargent, "The European Unemployment Dilemma," *, Journal of Political Economy*, 1988.

Lucas, Robert, "Asset Prices in an Exchange Economy," *Econometrica*, 1978, *46*, 1429–1446.

Ludvigson, Sydney C., Sai Ma, and Serena Ng, "Uncertainty and Business Cycles: Exogenous Impulse or Endogenous Response?," *American Economic Journal: Macroeconomics,* forthcoming, 2019.

McCracken, Michael W and Serena Ng, "FRED-MD: A monthly database for macroeconomic research," *Journal of Business & Economic Statistics*, 2016, *34* (4), 574–589.

McDonald, Robert and Daniel Siegel, "The Value of Waiting to Invest," *The Quarterly Journal of Economics*, 1986, *101* (4), 707–728.

McGrattan, Ellen R and Edward C Prescott, "A reassessment of real business cycle theory," *American Economic Review*, 2014, *104* (5), 177–82.

Miranda, Mario J and Paul L Fackler, *Applied computational economics and finance*, MIT press, 2004.

Mody, Ashoka and Milan Nedeljkovic, "Central Bank Policies and Financial Markets: Lessons from the Euro Crisis," *CESifo Working Paper*, 2018.

Parente, Stephen L, "Technology adoption, learning-by-doing, and economic growth," *Journal of economic theory*, 1994, *63* (2), 346–369.

Prescott, Edward C and Michael Visscher, "Organization capital," *Journal of political Economy*, 1980, *88* (3), 446–461.

Ramey, Garey and Valerie A Ramey, "Technology commitment and the cost of economic fluctuations," Technical Report, National Bureau of Economic Research 1991.

Shin, Minchul and Molin Zhong, "A new approach to identifying the real effects of uncertainty shocks," *Journal of Business & Economic Statistics*, 2018, pp. 1–13.

Veldkamp, Laura L, "Slow boom, sudden crash," *Journal of Economic theory*, 2005, *124* (2), 230–257.

Wachter, Jessica A, "Can time-varying risk of rare disasters explain aggregate stock market volatility?," *The Journal of Finance*, 2013, *68* (3), 987–1035.

Wong, Yu Fu, "Spatial Experimentation," 2020. Unpublished paper, Columbia University.

Appendix

5.1 1. Proof of Proposition 1

The first-order condition for the optimality of Δ is

$$\lambda(u-\Delta)-\theta\Delta-\beta\int V_1 dF=0, \tag{33}$$

and the first-order condition for the optimality of x is

$$\int(\varepsilon V_1+V_2)\,dF=0. \tag{34}$$

Solving for Δ.—The envelope theorem gives

$$V_1=-\lambda(u-\Delta)+\beta\int V_1 dF=-\theta\Delta, \tag{35}$$

where the second equality uses (33). Substituting into (33) we have

$$\lambda(u-\Delta)=\theta\Delta-\beta\theta\int\Delta' dF(\varepsilon). \tag{36}$$

We seek a solution of the form (9) where α is a constant to be solved for. If (9) holds, (36) reads

$$\begin{aligned}\lambda\alpha u &= \theta(1-\alpha)u-\beta\theta\int(1-\alpha)(\alpha u+x\varepsilon)\,dF(\varepsilon)\\ &= \theta(1-\alpha)u-\beta\theta(1-\alpha)\alpha u,\end{aligned}$$

which, after cancellation of u leaves a quadratic in α, namely $\theta(1-\alpha)-\beta\theta(1-\alpha)\alpha-\lambda\alpha=0$, or

$$\beta\alpha^2-\left(1+\beta+\frac{\lambda}{\theta}\right)\alpha+1=0. \tag{37}$$

This implicit function has the solution for α given in (10).

Solving for x.—The envelope theorem also gives

$$V_2=1+\beta\int V_2 dF=\frac{1}{1-\beta}. \tag{38}$$

The second equality follows because the right-hand side of (38) is a contraction map with at most one solution for V_2. Substituting from (9) into (35) and from there (in an updated form) into (34) gives

$$\begin{aligned}0 &= -\int\varepsilon\theta\Delta' dF+\frac{1}{1-\beta}\\ &= -\int\varepsilon\theta(1-\alpha)(\alpha u+x\varepsilon)\,dF+\frac{1}{1-\beta},\end{aligned} \tag{39}$$

because $\Delta' = (1-\alpha)\,u' = (1-\alpha)\,(\alpha u + x\varepsilon)$. But $E(\varepsilon u) = 0$, which leads to (8).

We must show that this function solves (7). Let us proceed with the method of undetermined coefficients. Since $V = aA - bu^2 + c$,

$$\begin{aligned} aA - bu^2 + c &= A - \psi u^2 + \beta \int \left(a\,(A+x) - b\,(u + x\varepsilon - \Delta)^2 + c\right) dF(\varepsilon) \\ &= A - \psi u^2 + \beta \int \left(a\,(A+x) - b\,(\alpha u + x\varepsilon)^2 + c\right) dF(\varepsilon) \\ &= A - \psi u^2 + \beta\,(a\,(A+x) + c) - \beta b \int (\alpha u + x\varepsilon)^2\, dF(\varepsilon) \\ &= A - \psi u^2 + \beta\,(a\,(A+x) + c) - \beta b \alpha^2 u^2 - \beta b x^2 \sigma^2. \end{aligned}$$

Equating coefficients: $a = 1 + a\beta$, $b = \psi + b\beta\alpha^2$, and $c = \beta\,(ax + c - bx^2\sigma^2)$, so that

$$a = \frac{1}{1-\beta}, \quad b = \frac{\psi}{1-\beta\alpha^2}, \text{ and } \quad c = \frac{\beta}{1-\beta}\left(ax - bx^2\sigma^2\right).$$

This leads to

$$V(u, A) = \frac{A}{1-\beta} - \frac{\psi}{1-\beta\alpha^2}u^2 + \frac{\beta\left(\frac{x}{1-\beta} - \left[\frac{\psi}{1-\beta\alpha^2}\right]x^2\sigma^2\right)}{1-\beta},$$

where $x = \frac{1}{\theta\sigma^2(1-\beta)(1-\alpha)}$. Then $V_2(u, A) = 1/(1-\beta)$ which is consistent with (38). It remains to be shown that $V_1(u, A)$ agrees with (35) and (9). Now, since $\psi = \frac{1}{2}\left(\lambda\alpha^2 + \theta\,(1-\alpha)^2\right)$, they agree only if

$$\frac{\psi}{1-\beta\alpha^2} = \frac{1}{2}\theta\,(1-\alpha),$$

i.e., if

$$\left(\frac{\lambda}{\theta}\alpha^2 + (1-\alpha)^2\right) = (1-\alpha)\left(1-\beta\alpha^2\right). \tag{40}$$

But from (37),

$$\frac{\lambda}{\theta} = \frac{1}{\alpha} + \beta\alpha - 1 - \beta.$$

Substitute for λ/θ into (40) to conclude that $V_1(u, A)$ is consistent with (35) and (9) if and only if

$$\left(\alpha + \beta\alpha^3 - \alpha^2 - \beta\alpha^2 + (1-\alpha)^2\right) = (1-\alpha)\left(1-\beta\alpha^2\right). \tag{41}$$

But expanding the left-hand side of (41) yields

$$\left(\alpha + \beta\alpha^3 - \alpha^2 - \beta\alpha^2 + 1 + \alpha^2 - 2\alpha\right) = \beta\alpha^3 - \beta\alpha^2 + 1 - \alpha.$$

Conversely, expanding the right-hand side of (41) yields

$$(1-\alpha)\left(1-\beta\alpha^2\right) = 1 - \alpha - \beta\alpha^2 + \beta\alpha^3.$$

Therefore (41) holds, and V is therefore given by (11).

2. Proof of Proposition 2 and of Corollaries 1 and 2

Note that we can re-write 13 as $MA(t)$ process

$$u_t = \alpha^t u_0 + x \sum_{s=0}^{t} \alpha^{t-s} \varepsilon_s.$$

As a result, we have

$$\begin{aligned}
u_{t+1}^2 - u_t^2 &= (u_{t+1} + u_t)(u_{t+1} - u_t) \\
&= \left\{ \left(\alpha^{t+1} + \alpha^t\right) u_0 + x \left\{ \sum_{s=0}^{t+1} \alpha^{t+1-s} \varepsilon_s + \sum_{s=0}^{t} \alpha^{t-s} \varepsilon_s \right\} \right\} \\
&\quad \left\{ \left(\alpha^{t+1} - \alpha^t\right) u_0 + x \left\{ \sum_{s=0}^{t+1} \alpha^{t+1-s} \varepsilon_s - \sum_{s=0}^{t} \alpha^{t-s} \varepsilon_s \right\} \right\} \\
&= \underbrace{\left\{ \left(\alpha^{t+1} + \alpha^t\right) u_0 + x \left\{ 2 \sum_{s=0}^{t} \alpha^{t-s} \varepsilon_s + \varepsilon_{t+1} \right\} \right\}}_{\zeta_1} \underbrace{\left\{ \left(\alpha^{t+1} - \alpha^t\right) u_0 + x \varepsilon_{t+1} \right\}}_{\zeta_2}.
\end{aligned}$$

This is product of two variables ζ_1 and ζ_2 that follow normal distributions

$$\begin{aligned}
\zeta_1 &\sim N\left(\left(\alpha^{t+1} + \alpha^t\right) u_0, x^2 \left\{ 4 \left[\frac{1 - \alpha^{2(t+1)}}{1 - \alpha^2} \right] + 1 \right\} \sigma^2 \right) \\
\zeta_2 &\sim N\left(\left(\alpha^{t+1} - \alpha^t\right) u_0, x^2 \sigma^2 \right).
\end{aligned}$$

It's worth noting that the product of two variables can be written as

$$XY = \frac{1}{4}(X+Y)^2 - \frac{1}{4}(X-Y)^2.$$

It follows that since $X = \zeta_1$ and $Y = \zeta_2$ are normal distribution

$$\begin{aligned}
\zeta_1 + \zeta_2 - 2\alpha^{t+1} u_0 &\sim N\left(0, 4x^2 \left[\left[\frac{1 - \alpha^{2(t+1)}}{1 - \alpha^2} \right] + 1 \right] \sigma^2 \right) = A \xi_t \\
\zeta_1 + \zeta_2 - 2\alpha^{t} u_0 &\sim N\left(0, 4x^2 \left[\frac{1 - \alpha^{2(t+1)}}{1 - \alpha^2} \right] \sigma^2 \right) = B \xi_t.
\end{aligned}$$

where ξ_t is a standard normal and

$$\begin{aligned}
A &= \sqrt{4x^2\sigma^2 \left[\frac{1 - \alpha^{2(t+1)}}{1 - \alpha^2} + 1 \right]} \\
B &= \sqrt{4x^2 \left[\frac{1 - \alpha^{2(t+1)}}{1 - \alpha^2} \right] \sigma^2}.
\end{aligned}$$

Therefore, we have

$$\begin{aligned}\zeta_1\zeta_2 &= \frac{1}{4}\left(A\xi_t + 2\alpha^{t+1}u_0\right)^2 - \frac{1}{4}\left(B\xi_t + 2\alpha^t u_0\right)^2 \\ &= \frac{1}{4}\left(\left[A\xi_t\right]^2 + \left[2\alpha^{t+1}u_0\right]^2 + 4\alpha^{t+1}u_0 A\xi_t\right) \\ &\quad -\frac{1}{4}\left(\left[B\xi_t\right]^2 + \left[2\alpha^t u_0\right]^2 + 4\alpha^t u_0 B\xi_t\right) \\ &= C + \frac{1}{4}\left[A^2 - B^2\right]\xi_t^2 + \left(\alpha A - B\right)\alpha^t u_0\xi_t,\end{aligned}$$

where the constant

$$C = \left(\alpha^{t+1}u_0\right)^2 - \left(\alpha^t u_0\right)^2.$$

Now note that

$$A^2 - B^2 = 4x^2\sigma^2,$$

this leads to

$$\zeta_1\zeta_2 = C + x^2\sigma^2\xi_t^2 + \left(\alpha A - B\right)\alpha^t u_0\xi_t.$$

We now have the growth distribution

$$g_t = x - \psi\left[C_t + x^2\sigma^2\xi_t^2 + \left(\alpha A - B\right)\alpha^t u_0\xi_t\right], \tag{42}$$

where $\xi_t \sim N(0,1)$ and A, B and C are as stated in the proposition.

Proof of Corollaries 1 and 2:

Now notice that we can re-write the growth distribution in Eqs. (42) as follows,

$$\begin{aligned}g_t &= D_0 - \psi x^2\sigma^2\left(\xi + D_1\right)^2 \\ &= D_0 - \psi x^2\sigma^2\left(\xi^2 + 2\xi D_1 + D_1^2\right) \\ &= D_0 - \psi x^2\sigma^2\xi^2 - 2\xi D_1\psi x^2\sigma^2 - \psi x^2\sigma^2 D_1^2\end{aligned}$$

Matching the coefficients, we have

$$\begin{aligned}-2D_1\psi x^2\sigma^2 &= -\psi\left(\alpha A - B\right)\alpha^t u_0 \\ D_0 - \psi x^2\sigma^2 D_1^2 &= x - \psi C_t\end{aligned}$$

or

$$\begin{aligned}D_1 &= \frac{\psi\left(\alpha A - B\right)\alpha^t u_0}{2x^2\sigma^2} \\ D_0 &= x - \psi C_t + \psi x^2\sigma^2 D_1^2.\end{aligned}$$

Now, $g_t = D_0 - \psi x^2 \sigma^2 (\xi + D_1)^2$ is a linear function of a noncentral chi-squared distribution, with the degree of freedom of 1 and the centrality parameter equal to D_1^2. Its mean and variance satisfy,[21]

$$\begin{aligned} E(\xi + D_1)^2 &= 1 + D_1^2 \\ Var(\xi + D_1)^2 &= 2\left(1 + 2D_1^2\right) \end{aligned}$$

Therefore, we have

$$\begin{aligned} E(g_t) &= D_0 - \psi x^2 \sigma^2 (1 + D_1) \\ &= x - \psi C_t + \psi x^2 \sigma^2 D_1^2 - \psi x^2 \sigma^2 \left(1 + D_1^2\right) \\ &= x - \psi C_t - \psi x^2 \sigma^2 \end{aligned}$$

as stated in the corollary, and

$$\begin{aligned} Var(g_t) &= \left[\psi x^2 \sigma^2\right]^2 2\left(1 + 2D_1^2\right) \\ &= 2\psi^2 \left(x^2 \sigma^2\right)^2 + \psi^2 \left[\psi (\alpha A - B) \alpha^t u_0\right]^2 \end{aligned}$$

as stated in the corollary.

The skewness satisfies,

$$Skewness(g_t) = -\psi x^2 \sigma^2 \left[\frac{2^{3/2}(1 + 3D_1^2)}{(1 + 2D_1^2)^{3/2}}\right]$$

which is decreasing in σ^2.

For quantiles, it's well-known that there are no closed-form expressions for chi-squared distribution but there exist an approximation from Result 26.4.32 on page 942 of Abramowitz and Stegun (1948) where the pth percentile of the noncentral chi-squared is,

$$\chi_p^2 \approx \left(1 + D_1^2\right) \left[1 - \frac{2(1 + 2D_1^2)}{9(1 + D_1^2)^2}\right]^3.$$

Plugging in D_1, we have

$$\begin{aligned} Median(g_{t+1}) &= x - \psi C_{t+1} - 0.47\psi \left(1 - \alpha^2\right) \tau \\ IQR(g_{t+1}) &= \chi_{75}^2 - \chi_{25}^2 \\ &= \psi \left(1.22 \left(1 - \alpha^2\right) \tau + 1.34 (\alpha A_t - B_t) \alpha^t u_0\right), \end{aligned}$$

as stated in the corollary.

[21] https://mathworld.wolfram.com/NoncentralChi-SquaredDistribution.html

Uncertainty shocks – we consider rises in σ^{-2} as positive shocks to uncertainty τ according to equation (14). Therefore, we consider,

$$\frac{\partial E\left(g_{t+1}^{p}\right)}{\partial \tau}=\frac{\partial E\left(g_{t+1}^{p}\right)}{\partial \sigma^{-2}}\frac{\partial \sigma^{-2}}{\partial \tau},$$

and analogously for other moments. Therefore, to show $\frac{\partial E\left(g_{t+1}^{p}\right)}{\partial \tau}<0$, it's sufficient to show $\frac{\partial E\left(g_{t+1}^{p}\right)}{\partial \sigma^{-2}}$ as $\frac{\partial \sigma^{-2}}{\partial \tau}>0$ according to equation (14). Now according to proposition 1, mean growth satisfies, $E\left(g_{t+1}\right)=x-\psi C_{t+1}-\psi x^{2}\sigma^{2}$, and therefore

$$\frac{\partial E\left(g_{t+1}^{p}\right)}{\partial \sigma^{-2}}=\frac{\partial x}{\partial \sigma^{-2}}-\psi\left(1-\alpha^{2}\right)\frac{\partial x^{2}\sigma^{2}}{\partial \sigma^{-2}}$$

because neither ψ nor C_{t+1} depend on σ^{-2}. Plugging in x from equation (8), we have

$$\frac{\partial E\left(g_{t+1}^{p}\right)}{\partial \sigma^{-2}}=\left[1-\frac{\psi}{\theta\left(1-\beta\right)\left(1-\alpha\right)}\right]\frac{1}{\theta\left(1-\beta\right)\left(1-\alpha\right)}\sigma^{-2},$$

so we have

$$\frac{\partial E\left(g_{t+1}^{p}\right)}{\partial \sigma^{-2}}<0 \text{ iff } 1<\frac{\psi}{\theta\left(1-\beta\right)\left(1-\alpha\right)}$$

or $\psi>\theta\left(1-\beta\right)\left(1-\alpha\right)$ as stated in the proposition 2. This inequality holds under parameters in Table 1.

The proofs for median, variance and IQR are similar. If $\psi>\theta\left(1-\beta\right)\left(1-\alpha\right)$

$$\begin{aligned}
\frac{\partial \mathbb{V}\left(g_{t+1}\right)}{\partial \sigma^{-2}} &= \frac{2\psi^{2}\left(1-\alpha^{2}\right)^{2}}{\left[\theta\left(1-\beta\right)\left(1-\alpha\right)\right]^{2}}\underbrace{\frac{\partial\left(\sigma^{-2}\right)^{2}}{\partial \sigma^{-2}}}_{>0}>0\\
\frac{\partial Median\left(g_{t+1}\right)}{\partial \sigma^{-2}} &= \left[\underbrace{0.47-\frac{\psi}{\theta\left(1-\beta\right)\left(1-\alpha\right)}}_{<0 \text{ if } \psi>\theta(1-\beta)(1-\alpha)}\right]\frac{1}{\theta\left(1-\beta\right)\left(1-\alpha\right)}<0\\
\frac{\partial IQR\left(g_{t+1}\right)}{\partial \sigma^{-2}} &= 1.22\psi\left(1-\alpha^{2}\right)\underbrace{\frac{\partial \tau}{\partial \sigma^{-2}}}_{>0}>0
\end{aligned}$$

as stated in the Proposition 2.

Limit: As $t\to\infty$, we have $\alpha^{t}\to 0$ because $\alpha\in(0,1)$ and hence $C_{t}\to 0$, we thus achieve the limits of the moments stated in the Corollary 2.

3. Proof of Proposition 3 and Corollary 3

Proof of Proposition 3: There are four first-order conditions. The first-order condition for the optimality of Δ_i in state $i \in \{\text{L, H}\}$ is

$$\lambda (u - \Delta_i) - \theta \Delta_i - \beta \int \left(p V'_{u,i} + (1-p) V'_{u,j} \right) dF_{\text{i}} = 0, \tag{43}$$

Solving for Δ_i.—The envelope theorem gives

$$V_{u,i} = -\lambda (u - \Delta_i) + \beta \int \left(p V'_{u,i} + (1-p) V'_{u,j} \right) dF_{\text{i}} = -\theta \Delta_i, \tag{44}$$

where the second equality uses (43). Substituting $V'_{u,i} = -\theta \Delta'_i$,into (43) we have

$$\lambda (u - \Delta_i) = \theta \Delta_i - \beta \theta \int \left(p \Delta'_i + (1-p) \Delta'_j \right) dF_i. \tag{45}$$

We seek a solution of the form (9), so that where (α_1, α_2) are constants to be solved for. If (27) holds, (45) reads

$$\begin{aligned} \lambda \alpha_i u &= \theta (1 - \alpha_i) u - \beta \theta \int (1 - \alpha_i) (\alpha_i u + x_i \varepsilon) \, dF(\varepsilon) \\ &= \theta (1 - \alpha_i) u - \beta \theta (1 - \alpha_i) \alpha_i u, \end{aligned}$$

which is an equation in α_i alone, of the same form as Eq. (37), and with the same solution $\alpha_{\text{L}} = \alpha_{\text{H}} = \alpha$, with α given in (10). This proves Eq. (9).

Solving for x_i.—The first-order condition for the optimality of x_i for $i \in \{\text{L, H}\}$ is

$$\int \left[p (\varepsilon V_{u,i} + V_{A,i}) + (1-p) \left(\varepsilon V'_{u,j} + V'_{A,j} \right) \right] dF_{\text{i}} = 0. \tag{46}$$

The envelope theorem also gives

$$V_{A,\,i} = 1 + \beta \int \left(p V_{A,i} + (1-p) V_{A,j} \right) dF_{\text{i}} = \frac{1}{1-\beta}. \tag{47}$$

Substituting $V'_{u,i} = -\theta \Delta'_i$ and $V'_{A,i} = 1/(1-\beta)$ into Eq. (46) and rearranging, it reads

$$\frac{1}{1-\beta} = \int \left[p \varepsilon \theta \Delta'_i + (1-p) \varepsilon \theta \Delta'_j \right] dF_{\text{i}}.$$

Now $\Delta'_i = \Delta'_j = (1-\alpha) u = (1-\alpha) (\alpha u + x_i \varepsilon)$. And since ε has zero mean, we are left with

$$\frac{1}{1-\beta} = \int \left[p\theta + (1-p) \theta \right] (1-\alpha) x_i \varepsilon^2 dF_{\text{i}} = \theta (1-\alpha) x_i \sigma_i^2,$$

implying Eq. (26). That completes the proof of the Proposition.

Proof of Corollary 3: The growth for state $i \in \{L, H\}$ can be expressed as

$$\begin{aligned} g_i &\equiv \ln y' - \ln y = x_i - \psi\left(u'^2 - u^2\right). \\ &= x_i - \psi\left((\alpha u + x_i\varepsilon)^2 - u^2\right) \\ &= \left[x_i + \psi\left(1-\alpha^2\right)u^2\right] + 2\psi\alpha u x_i \sigma_i \xi - \psi x_i^2 \sigma_i^2 \xi^2, \end{aligned}$$

i.e., Eq. (28)

4. Proof of Proposition 4 and Corollary 4

Proof of Proposition 4: Because we can express the total output as

$$\ln y_t^p = A_0 + xt - \frac{\lambda}{2}\alpha^2 u_t^2,$$

it's straightforward to see that the proof of proposition 2 goes through in this case when we replace ψ by $\frac{\lambda}{2}\alpha^2$. Therefore the growth distribution satisfies,

$$g_t = x - \frac{\lambda}{2}\alpha^2\left[C_t + x^2\sigma^2\xi_t^2 + \left(\alpha A - B\right)\alpha^t u_0 \xi_t\right]$$

with

$$\begin{aligned} A_t &= \sqrt{4\left(1-\alpha^2\right)\tau\left(\frac{1-\alpha^{2t}}{1-\alpha^2}+1\right)} \\ B_t &= \sqrt{4\left(1-\alpha^2\right)\tau\left(\frac{1-\alpha^{2t}}{1-\alpha^2}\right)} \\ C_t &= \left(\alpha^t u_0^p\right)^2 - \left(\alpha^{t-1}u_0^p\right)^2 \\ u_0^p &= \sqrt{\left(\frac{\lambda}{2}\alpha^2\right)^{-1}\left(\ln y_0 - A_0\right)^2}. \end{aligned}$$

In equilibrium, the distribution of growth g_{t+1} therefore satisfies

$$\begin{aligned} E\left(g_{t+1}^p\right) &= x - \frac{\lambda}{2}\alpha^2 C_{t+1} - \frac{\lambda}{2}\alpha^2\left(1-\alpha^2\right)\tau \\ Median\left(g_{t+1}^p\right) &= x - \frac{\lambda}{2}\alpha^2 C_{t+1} - 0.47\left(\frac{\lambda}{2}\alpha^2\right)\left(1-\alpha^2\right)\tau \\ \mathbb{V}\left(g_{t+1}^p\right) &= 2\left(\frac{\lambda}{2}\alpha^2\right)^2\left(1-\alpha^2\right)^2\tau^2 + \left(\frac{\lambda}{2}\alpha^2\right)^2\left(\left(\alpha A_{t+1} - B_{t+1}\right)\alpha^t u_0^p\right)^2 \\ IQR\left(g_{t+1}^p\right) &= \frac{\lambda}{2}\alpha^2\left(1.22\left(1-\alpha^2\right)\tau + 1.34\left(\alpha A_t - B_t\right)\alpha^t u_0^p\right). \end{aligned}$$

Proof of Corollary 4:

Therefore we have,

$$\frac{\partial E\left(g_{t+1}^{p}\right)}{\partial\tau}<0,\ \frac{\partial Median\left(g_{t+1}^{p}\right)}{\partial\tau}<0,\frac{\partial\mathbb{V}\left(g_{t+1}^{p}\right)}{\partial\tau}>0,\ \frac{\partial IQR\left(g_{t+1}^{p}\right)}{\partial\tau}>0.$$

The 5th percentile, or the growth-at-risk, satisfies

$$\chi_{t}^{p}=x-\frac{\lambda}{2}\alpha^{2}C_{t+1}-3.84\left(\frac{\lambda}{2}\alpha^{2}\right)\left(1-\alpha^{2}\right)\tau+1.65\left(\frac{\lambda}{2}\alpha^{2}\right)\left(\alpha A_{t+1}-B_{t+1}\right)\alpha^{t}u_{0}^{p},\quad(48)$$

and because $\alpha\in(0,1)$, we thus have

$$\frac{\partial\chi_{t}^{p}}{\partial\tau}=-3.84\left(\frac{\lambda}{2}\alpha^{2}\right)\left(1-\alpha^{2}\right)<0$$

as stated in the corollary.

5. Proof of Proposition 5 and Corollary 5 (Recursive Preferences)

Proof of Proposition 5: We guess that the value function takes the following form,

$$V\left(u,A\right)=e^{A}v\left(u\right).\quad(49)$$

To verify this guess, we plug the guess into the RHS of value function (31), and it becomes

$$\begin{aligned}\text{RHS} &= \max_{x,\Delta}\left[e^{(1-\phi)A}\exp\left\{-\frac{\lambda}{2}\left(u-\Delta\right)^{2}-\frac{\theta}{2}\Delta^{2}\right\}^{1-\phi}+\beta\left[\int e^{(A+x)}v\left(u+x\varepsilon-\Delta\right)^{1-\gamma}dF\right]^{\frac{1-\phi}{1-\gamma}}\right]^{\frac{1}{1-\phi}}\\ &= \underbrace{e^{A}\max_{x,\Delta}\left[\exp\left\{-\frac{\lambda}{2}\left(u-\Delta\right)^{2}-\frac{\theta}{2}\Delta^{2}\right\}^{1-\phi}+\beta e^{(1-\phi)x}\left[\int v\left(u+x\varepsilon-\Delta\right)^{1-\gamma}dF\right]^{\frac{1-\phi}{1-\gamma}}\right]^{\frac{1}{1-\phi}}}_{v(u)}.\end{aligned}$$

As a result, the RHS of value function (31) can be expressed as $e^{A}v\left(u\right)$ where

$$v\left(u\right)=\max_{x,\Delta}\left[\exp\left\{-\frac{\lambda}{2}\left(u-\Delta\right)^{2}-\frac{\theta}{2}\Delta^{2}\right\}^{1-\phi}+\beta e^{(1-\phi)x}\left[\int v\left(u+x\varepsilon-\Delta\right)^{1-\gamma}dF\right]^{\frac{1-\phi}{1-\gamma}}\right]^{\frac{1}{1-\phi}}.\quad(50)$$

which is exactly our guess. Because the RHS of equation (50) is independent of A, so are optimal policy functions (x,Δ).

Proof of Corollary 5: When $\gamma=\phi$, we can re-write $v\left(u\right)$ from equation (50) as

$$v\left(u\right)=\max_{x,\Delta}\left[\exp\left\{-\frac{\lambda}{2}\left(u-\Delta\right)^{2}-\frac{\theta}{2}\Delta^{2}\right\}^{1-\phi}+\beta e^{(1-\phi)x}\left[\int v\left(u+x\varepsilon-\Delta\right)^{1-\gamma}dF\right]\right]^{\frac{1}{1-\phi}},$$

therefore, we have

$$\frac{v(u)^{1-\phi}}{1-\phi} = \max_{x,\Delta} \frac{\exp\left\{-\frac{\lambda}{2}(u-\Delta)^2 - \frac{\theta}{2}\Delta^2\right\}^{1-\phi}}{1-\phi} + \beta e^{(1-\phi)x}\left[\int \frac{v(u+x\varepsilon-\Delta)^{1-\gamma}}{1-\gamma} dF\right].$$

When $\gamma = \phi \to 1$, we have $\frac{v(u)^{1-\phi}}{1-\phi} \to \ln v(u)$, and therefore we have

$$\ln v(u) = \max_{x,\Delta} -\frac{\lambda}{2}(u-\Delta)^2 - \frac{\theta}{2}\Delta^2 + \beta\left[\int \ln\left(v(u+x\varepsilon-\Delta)\right) dF\right].$$

As a result,

$$\begin{aligned} \ln V_{EZ}(u,A) &= A + \ln(v(u)) \\ &= \max_{x,\Delta}\ A - \frac{\lambda}{2}(u-\Delta)^2 - \frac{\theta}{2}\Delta^2 + \beta\left[\int \ln V_{EZ}(u+x\varepsilon-\Delta, A+x)\, dF\right] \end{aligned}$$

which is the same as (7) with,

$$V(u,A) = \ln V_{EZ}(u,A).$$

Therefore, using results from Proposition 1, we have

$$\ln V_{EZ}(u,A) = \frac{A}{1-\beta} - \frac{1}{2}\theta(1-\alpha)u^2 + J$$

where J satisfies equation (12).

Numerical Procedure for Computation of $x_{EZ}(u)$ and $\alpha_{EZ}(u)$: We guess and verify numerically that

$$v(u) = D_0 e^{D_1 u^2} \tag{51}$$

where D_0 and D_1 are two constants remained to be solved. Using the guess and substitute $\alpha = 1 - \frac{\Delta}{u}$, $v(u)$ can be expressed as

$$v(u)^{1-\phi} = \max_{x,\alpha}\left[\begin{array}{c} \exp\left\{(1-\phi)\left(-\frac{\lambda}{2}\alpha^2 - \frac{\theta}{2}(1-\alpha)^2\right)u^2\right\} \\ +\beta e^{(1-\phi)x} D_0^{1-\phi}\left[\int e^{(1-\gamma)D_1(\alpha u + x\sigma Z)^2} d\Phi(Z)\right]^{\frac{1-\phi}{1-\gamma}} \end{array}\right] \tag{52}$$

where Z follows $N(0,1)$ and $\Phi(Z)$ is the CDF of Z. The integral $\int e^{(1-\gamma)D_1(\alpha u + x\sigma Z)^2} d\Phi(Z)$, which is the expectation of the exponential of a noncentral chi-squared distribution, has no closed-form solution. Therefore, we numerically calculate this integral by using the "qnwnorm" function in the Matlab CompEcon toolbox from Miranda and Fackler (2004).

Next, for any given pair $(D_{0,}D_1)$, we numerically calculate the optimal (x,α) that maximize RHS of equation (52) which restricts $\alpha \in (0,1)$ and $x \in (0, x_{\max})$. The upper bound $x_{\max}$ is set to make sure the optimal solutions are interior points. Last, at the optimal (x,α), we compute the value function, denoted by $v^{\text{Num}}(u; D_{0,}D_1)$. The algorithm stops if we find a pair (D_0, D_1) that satisfies $\frac{1}{N_u}\sum_u \left(v^{\text{Num}}(u; D_{0,}D_1) - D_0 e^{D_1 u^2}\right)^2 < 10^{-2}$ where N_u is the size of the grid of u.

6. Out-of-sample Predictive Scores

In this section, we evaluate the forecast performance of our empirical quantile regression with JLN uncertainty and compare it to the one from Adrian et al. (2019). Following Adrian et al. (2019), we evaluate the out-of-sample prediction performance among different models using predictive scores. The predictive scores are computed as the predictive distribution generated by a model and then evaluated at the realized value of the time series. By construction, higher predictive scores are indicative of a more accurate forecast. We produce the predictive distributions recursively starting with the sample ranging from 1971:01 to 1994:12 to predict growth distribution for 1995:01 by estimating quantile regressions (1) and then matching a skewed t-distribution. We then repeat the exercise for 1995:02 by expanding the estimation sample to 1995:01, and so on until reaching the end of the sample at 2018:12.

We consider three alternative models. The first one is our baseline model using JLN uncertainty as the predictor. The second is the one studied in Adrian et al. (2019), which uses NFCI. The third model includes both JLN uncertainty and NFCI. In all models, we include the contemporaneous IP growth as the second predictor. Table A1 reports the average predictive scores for each model for $h = 1$ and 12 month-ahead forecasts. Our baseline model with JLN uncertainty produces the highest average out-of-sample predictive score among the three models; it outperforms the NFCI model out-of-sample. Interestingly, when we add NFCI to the baseline model, the out-of-sample prediction performance decreases, which shows that JLN uncertainty brings additional predictive power over NFCI for predicting future IP growth.

Table A1. Out-of-sample Predictive Scores

Model	Predictive Scores	
	$h = 1$	$h = 12$
JLN Uncertainty Only	0.0447	0.1061
NFCI	0.0439	0.1004
JLN Uncertainty + NFCI	0.0431	0.0998

Note: This table reports the average predictive scores from 1995:01 to 2018:12.